Progress in Neurobiology 258 (2026) 102881

Contents lists available at ScienceDirect

Progress in Neurobiology

journal homepage: www.elsevier.com/locate/pneurobio

Sustained inhibitory dysfunction in complement component C1qa-deficient mice underlies epilepsy and comorbidities

Joseane Righes Marafiga [a,*], Thy Vu [a], Jessica Bowlus [a], Scott C. Baraban [a,b,1,**]

[a] Department of Neurological Surgery, University of California San Francisco, San Francisco, CA 94143, United States
[b] Helen Wills Institute for Neuroscience, University of California Berkeley, Berkeley, CA 94720, United States

ARTICLE INFO

Keywords:
C1qa loss
epilepsy
somatostatin interneurons
cortical dysfunction
electrophysiology

ABSTRACT

Neuronal networks undergo critical refinement throughout development and adulthood to maintain proper brain function. Dysregulation of complement component C1qa—including both up- and downregulation—has been linked to circuit dysfunction and neurological disorders such as epilepsy, primarily through effects on excitatory synapses. However, the impact of C1qa downregulation on inhibitory circuits remains poorly understood. We show that germline deletion of C1qa disrupts layer 6 somatostatin (SST)-expressing interneurons in the somatosensory cortex, which we propose underlies enhanced excitatory synaptic transmission, electrographic spike-and-wave discharges, anxiety-like behavior, and impaired sensory-driven behavior. Transplantation of medial ganglionic eminence (MGE)-derived interneuron precursors rescued behavioral deficits but did not abolish the seizure phenotype, underscoring the critical role of C1qa in maintaining inhibitory network integrity—while also suggesting that additional mechanisms beyond interneuron dysfunction contribute to the pathophysiology of absence seizures.

1. Introduction

The establishment of functional neuronal circuits relies on tightly orchestrated processes of synaptic development and refinement that begin early in postnatal life (Hensch, 2004; Tau and Peterson, 2010). During this critical window, perturbations in molecular signaling, neuronal function, and synaptic connectivity can impair maturation of network architecture, resulting in long-lasting alterations that contribute to emergence of debilitating neurodevelopmental disorders (Tau and Peterson, 2010). Epilepsy, one of the most common pediatric neurological conditions (Aaberg et al., 2017), frequently arises during these early developmental periods, coinciding with dynamic changes in synaptic structure and circuit excitability (Clement et al., 2013).

Increasing evidence implicates components of the classical complement cascade, particularly the initiating molecule C1q, in developmental refinement of neural circuits (Stevens et al., 2007). C1q is canonically involved in activity-dependent synaptic pruning, a process by which excess or weak synapses are eliminated to enhance circuit efficiency. Under physiological conditions, C1q-mediated synaptic pruning restrains hyperexcitability and supports circuit stability (Chu et al., 2010). Paradoxically, in neurological diseases, such as Alzheimer's disease (Dejanovic et al., 2022; Tenner, 2020), Huntington's disease (Wilton et al., 2023) and schizophrenia (Yilmaz et al., 2021), upregulation of this same pathway has been linked to pathological synapse loss (Carvalho et al., 2019; Dejanovic et al., 2022; Presumey et al., 2017), neuroinflammation (Madeshiya et al., 2022; Wu et al., 2023), and progressive network dysfunction (Stephan et al., 2013).

In drug-resistant epilepsy patients, C1q expression is upregulated in resected brain tissue (Wyatt et al., 2017). Preclinical models similarly implicate complement components, including C1q and C3, in promoting circuit hyperexcitability and facilitating epileptogenesis (Aronica et al., 2007; Holden et al., 2021; Jeong et al., 2025; Schartz et al., 2018). Down-regulation of C1q, through function blocking antibody administration in both a mouse model of traumatic brain injury and in an acquired epilepsy model, has demonstrated anti-epileptic activity (Holden et al., 2021; Jeong et al., 2025). On the other hand, germline deletion of

Abbreviations: SST, somatostatin-expressing interneurons; PV, parvalbumin-expressing interneurons; SWD, spike-and-wave discharges; AE, absence-epilepsy; EPSC, excitatory post-synaptic currents; IPSC, inhibitory post-synaptic currents; MGE, medial ganglionic eminence; KO, knockout; WT, wild-type.

* Corresponding author.
** Corresponding author at: Department of Neurological Surgery, University of California San Francisco, San Francisco, CA 94143, United States.
E-mail addresses: joseane.righesmarafiga@ucsf.edu (J. Righes Marafiga), scott.baraban@ucsf.edu (S.C. Baraban).
[1] Lead contact

https://doi.org/10.1016/j.pneurobio.2026.102881
Received 9 July 2025; Received in revised form 6 January 2026; Accepted 13 January 2026
Available online 14 January 2026

C1qa in mice leads to spontaneous absence-like seizures, cortical hyperexcitability, and excessive arborization of excitatory circuits during early postnatal development (Chu et al., 2010; Ma et al., 2013). The conflicting and potentially bidirectional consequences of complement dysregulation highlight the need to resolve cell type and stage-specific mechanisms by which individual complement components shape circuit development and influence epileptogenesis. Because of these opposing results, we sought to define mechanisms by which C1qa deletion impacts circuit function and the emergence of electrographic seizure-like activity. While enhanced excitatory synaptic input has been implicated in the hyperexcitability observed in C1qa-deficient mice (Chu et al., 2010), it remains unclear whether this alone accounts for the phenotype. Could downregulation of complement cascade also alter inhibitory circuit maturation, driving persistent network dysfunction and increased seizure susceptibility?

Disruption of interneuron development or inhibitory synaptic integration - particularly of parvalbumin (PV)- and somatostatin (SST)-expressing interneurons - can impair inhibitory control of pyramidal networks, leading to cortical hyperexcitability, hypersynchrony, and seizures (Righes Marafiga et al., 2021). Given the timing of complement components expression and its established role in synaptic elimination, a failure to properly sculpt GABAergic networks could result in a persistent excitation–inhibition imbalance (Chen et al., 2025). Characterizing how C1qa deficiency affects inhibitory synapses may uncover additional mechanisms by which altered network homeostasis drives absence-like seizures in C1qa knockout (KO) mice.

Thus motivated, we investigated whether germline deletion of C1qa disrupts development of inhibitory neurons, resulting in persistent network alterations that not only initiate epileptogenesis during early life but also destabilize circuits into adulthood. Centered on inhibitory circuit dynamics, our findings identify somatostatin interneurons as a key link between complement-mediated neuronal circuit disruption and enduring neurobehavioral dysfunction, while absence-seizures generation in C1qa-deficient mice appears to emerge from network-level processes beyond inhibitory failure.

2. Results

2.1. Adult C1qa KO mice show spontaneous spike-and-wave discharges and cortical hyperexcitability

Although previous studies using C1q-deficient mice reported beneficial effects of C1q deletion in murine models of neurological diseases (Schulz and Trendelenburg, 2022; Zhang et al., 2023), C1qa KO mice exhibit spontaneous absence-like seizures during developmental periods corresponding to early childhood and adolescence in humans (e.g., P18–27). These seizures, marked by bi-hemispheric spike-and-wave discharges (SWDs) and behavioral arrest, are consistent with electroclinical features of absence epilepsy (Chu et al., 2010). Whether the absence epilepsy phenotype observed in C1qa KO mice persists in adulthood or is accompanied by emerging comorbidities remains unclear.

To address this issue, we first performed chronic *in vivo* EEG recordings from the somatosensory cortex of C1qa KO mice (24 h per day, 5 days per week) during periods of quiet wakefulness. C1qa KO mice, starting at 2 months old, exhibited frequent and stereotyped SWDs, averaging 39 ± 8 events per hour (Fig. 1B), with a mean duration of 11.1 ± 10 s (Fig. 1D). Representative traces of SWDs dominant activity

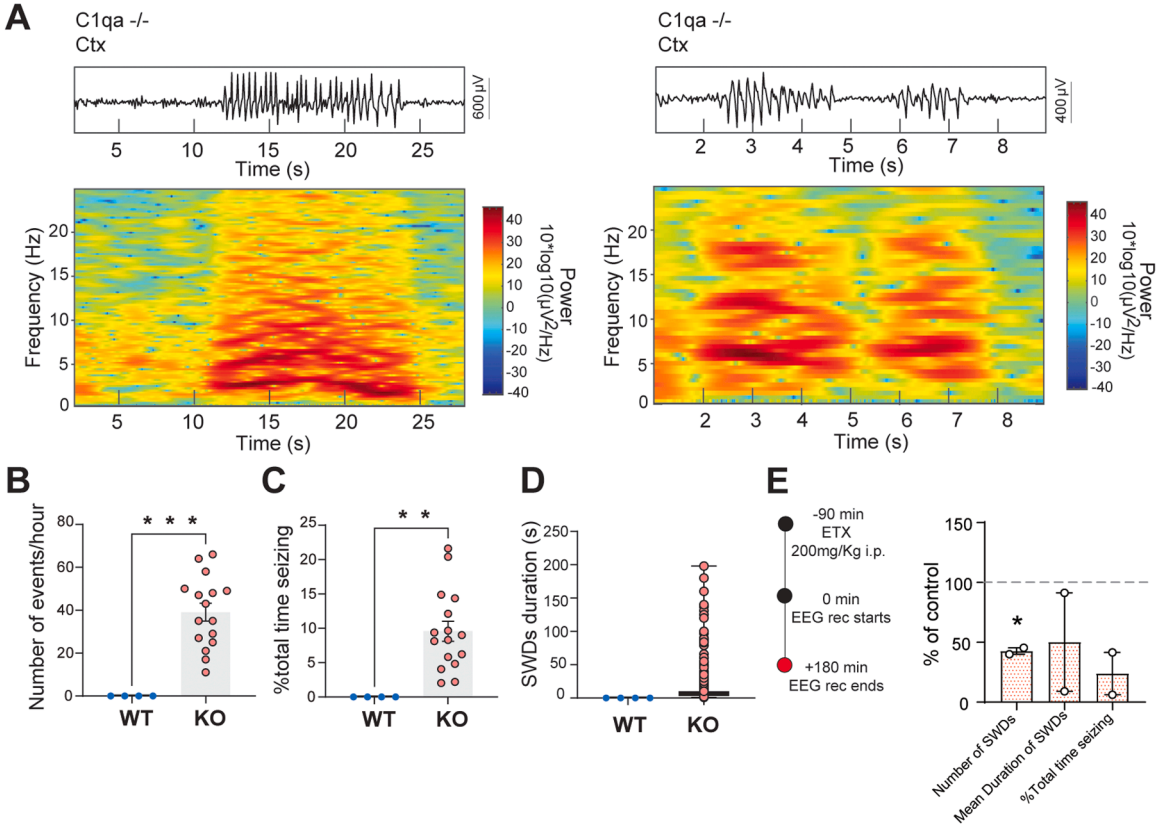

Fig. 1. Spontaneous spike-and-wave discharges (SWDs). (A) Representative EEG traces from somatosensory cortex of a C1qa KO mouse showing stereotyped SWDs centered around 5 Hz (KO: 9 mice, 18 epochs 1 h/epoch). **(B)** Quantification of SWD frequency during quiet wakefulness. **(C)** Percentage of time spent seizing. **(D)** Mean SWD duration. *p < 0.05, two-tailed unpaired *t* test. **(E)** Ethosuximide treatment in C1qa KO mice partially reduced SWD frequency, duration, and time spent seizing (KO: 2 mice, 2 epochs 1 h/epoch). Data is shown as percentage of control (KO previously to ethosuximide administration). *p < 0.05, one-sample t test (KO naive: 100 %). WT mice exhibited no SWDs under the same recording conditions and were not displayed (WT: 4 mice).

centered around 5 Hz are shown in Fig. 1A. Consistent with an epileptic phenotype, implanted C1qa KO mice spent approximately 9.56 ± 2.98 % of their wakeful time in absence seizure-like activity (Fig. 1C), though this proportion was somewhat lower than previously reported in early stages of development (Chu et al., 2010). To validate the presence of spontaneous SWDs, we administered a single acute intraperitoneal dose of ethosuximide, a T-type calcium channel antagonist commonly used to treat absence epilepsy (Le Roux et al., 2024). Ethosuximide significantly reduced SWD frequency (42.73 ± 2.72 % of control), but did not produce a statistically significant effect on SWD duration (50.23 ± 41.15 % of control) or total time spent in seizures (23.88 ± 17.68 % of control) (Fig. 1E), consistent with the limited and variable efficacy of antiepileptic therapy in managing absence seizures in some patients (Glauser et al., 2013). SWDs or similar EEG abnormalities were never observed in WT mice (Table S1).

To further evaluate how loss of C1qa affects synaptic transmission during later stages of adulthood, we performed whole-cell patch-clamp recordings in acute coronal slices from WT and C1qa KO mice starting at 2 months of age. This question is particularly relevant, as the functional consequences of C1qa deletion beyond early developmental windows remain incompletely understood. Analysis focused on spontaneous excitatory and inhibitory postsynaptic currents (sEPSCs and sIPSCs, respectively) recorded from layer 2/3 and layer 5/6 pyramidal neurons in the somatosensory cortex. We found that C1qa KO mice exhibited a significant increase in sEPSC amplitude (Fig. 2A-B) and impaired sEPSC rise-time 10–90 of L2/3 pyramidal cells (Fig. 2A,E), while L5/6 pyramidal cells showed increased sEPSC amplitude and frequency compared to age-matched WT controls (Fig. 2F–H), with no changes in sEPSC kinetics (Fig. 2F, I, J, Table S2). These findings indicate that early alterations in excitatory synaptic transmission in C1qa KO mice (Chu et al., 2010) persist into later stages of maturation and adulthood and are extended to the superficial layers of somatosensory cortex. No significant differences were observed in sIPSC amplitude, frequency, or kinetics between C1qa KO and WT mice (Fig. 2K-T, Table S2) in either superficial or deep layers of somatosensory cortex.

Together, these findings indicate that C1qa deficiency leads to generalized, long-term disruption in excitatory synaptic transmission and absence seizure–like activity that extend beyond the critical period of CNS development.

2.2. Selective decrease in somatostatin interneuron density in mature adult C1qa KO mice

Loss of the complement cascade protein C1q in mice impairs refinement of central nervous system (CNS) synapses. This disruption occurs in developing brain regions during the critical period of synaptic pruning and appears to affect excitatory synapses in cortex (Yuzaki, 2017). However, the extent to which C1qa loss affects inhibitory circuitry remains largely unexplored.

Given that changes in interneuron density can disrupt local network dynamics and potentially influence long-range connectivity underlying epileptic phenotypes (Righes Marafiga et al., 2021), we investigated whether C1qa loss affects the two major cortical interneuron subtypes innervating soma and dendritic regions of excitatory pyramidal neurons: parvalbumin- (PV) and somatostatin-expressing (SST) interneurons, respectively. To this end, we quantified PV and SST interneuron density in somatosensory cortex of C1qa KO mice at two and five months of age (Fig. 3, Table S3).

We found that, at two months old, C1qa KO mice show a decreased SST-INs density restricted to layer 6 (Figs. 3A, 3C-G). The total number of SST-INs across all layers was not different between C1qa KO and WT mice (Fig. 3D). At 5 months, C1qa KO mice also showed decreased SST-INs in layer 6 (Fig. 3L), and an overall decrease of SST-INs in SS cortex (Figs. 3B and 3H-I). No significant differences were found between these two different ages (Table S3).

In contrast, PV-INs were homogeneously expressed within all somatosensory cortical layers, showing no significant differences between C1qa KO and WT control mice on overall density or in layer-specific analyses (Fig. S1A-J). PV-INs did not differ between young adult and mature adult ages (Table S3, Fig. S1). Our findings identify a novel, cell type–specific effect of C1qa loss, marked by reduced SST-expressing interneuron density in the somatosensory cortex.

2.3. Somatosensory-related behavior impairment in C1qa deficient mice

Although we observed circuit-level impairments and spontaneous absence seizure–like activity in C1qa KO mice, we sought additional evidence to evaluate whether these circuit-level disruptions translate into functional behavioral impairments. To investigate this, we first performed the Textured Novel Object Recognition Test (tNORT), a whisker-dependent behavioral assay that relies on intact primary somatosensory cortex processing and has been shown to be sensitive to somatosensory dysfunction (Balasco et al., 2022a; Balasco et al., 2022b; Hayashi et al., 2024).

C1qa KO mice exhibited a significantly reduced discrimination index (DI) during the testing session compared to WT controls (Fig. 4A-D), indicating impaired textured object recognition. No significant differences were observed in the preference index (PI) during either training or testing phases (Figs. 4E and 4F), suggesting no innate bias toward textured objects. Interestingly, C1qa KO mice also spent less 'total time' exploring the objects (Figs. 4G and 4H), although the number of explorations did not differ between genotypes (Figs. 4I and 4J). Together, these findings suggest that C1qa KO mice exhibit reduced whisker-guided exploration and impaired texture discrimination (Table S4), likely suggesting a circuit-level dysfunction in the somatosensory cortex that compromises sensory-driven behavior.

Because tNORT evaluates spontaneous whisker-dependent exploration, we next tested responses to active whisker stimulation using the Whisker Nuisance (WN) test (Balasco et al., 2019). C1qa KO and WT mice were behaviorally scored based on their responses to whisker stimulation. No significant differences were observed in WN scores between KO and WT groups across the four test trials (Table S5, Fig. S2A). Additionally, there were no statistical differences between genotypes in individual behavioral parameters, including fearfulness, stance, breathing/hyperventilation, general responsiveness, and evasiveness (Fig. S2B).

Altogether, these findings suggest that while C1qa KO mice maintain normal sensory processing and a preserved tactile response during externally driven behaviors, they display circuit-level impairments in somatosensory cortical integration and spontaneous whisker-guided exploration of textured objects, as revealed by the tNORT.

2.4. Adult C1qa KO mice display behavioral comorbidities beyond somatosensory cortical abnormalities

Absence seizures are frequently associated with subtle cognitive deficits, language impairments, social difficulties, and an increased incidence of psychiatric conditions, most notably attention deficit hyperactivity disorder and anxiety (Caplan et al., 2008). To assess whether adult C1qa KO mice display behavioral comorbidities reminiscent of those observed in patients with epilepsy (Kwon et al., 2025; Patrikelis et al., 2009; Vinti et al., 2021), we performed a battery of five standardized behavioral assays targeting locomotor activity, anxiety-like behavior, social interaction, stereotyped behavior, and depressive-like responses, both tests that reflect domains commonly affected in these patients.

To evaluate anxiety-like behavior, we performed a dark/light preference testing paradigm (Fig. 5A, C-E, Table S6) (Bourin and Hascoët, 2003). Time spent in light zone and number of crossings between zones were scored, demonstrating that C1qa KO mice exhibit decreased time spent in the light zone (Fig. 5C), and lower number of light/dark chamber crossings (Fig. 5D), suggesting increased anxiety-like behavior.

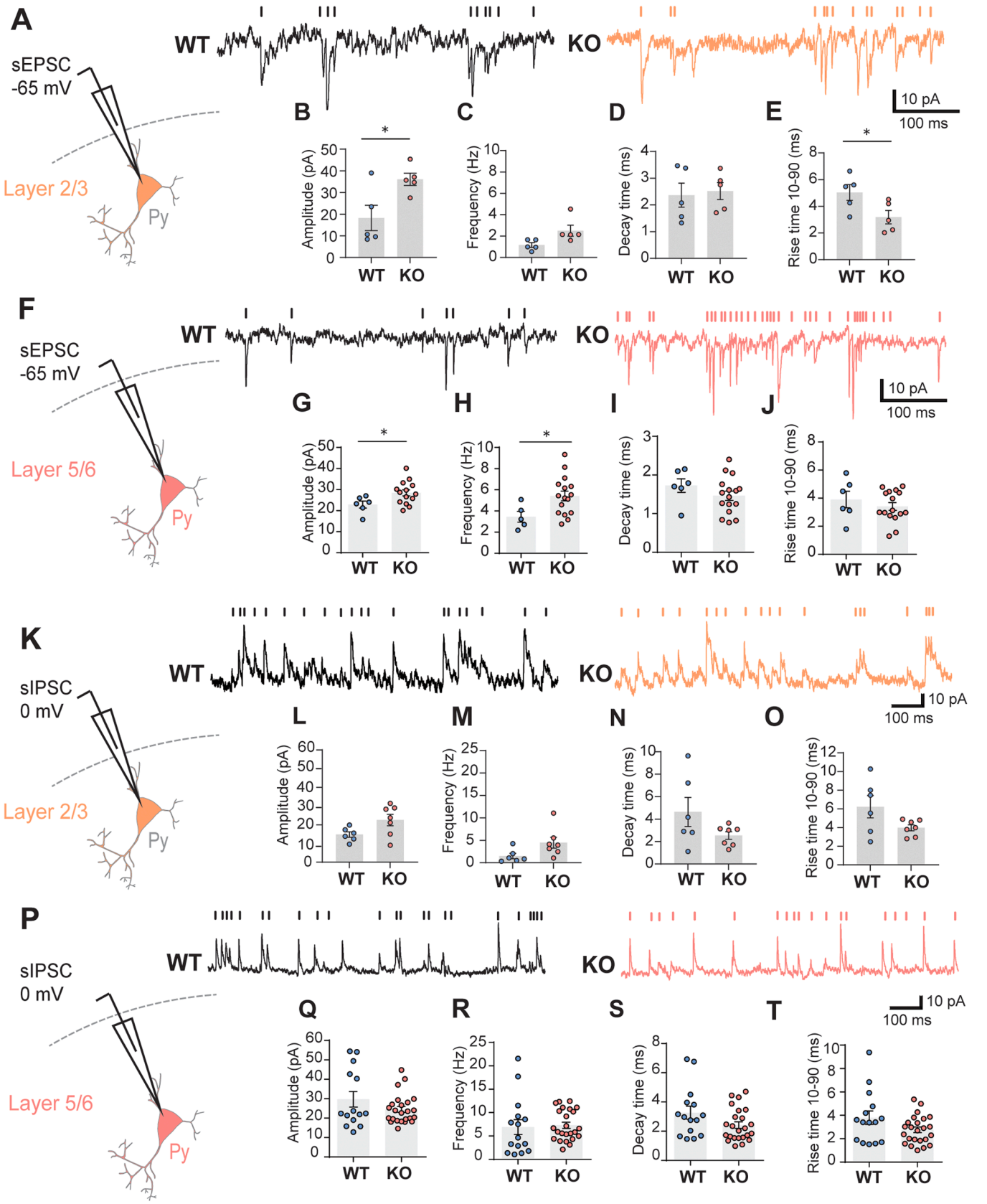

(caption on next page)

Fig. 2. Increased spontaneous excitatory synaptic transmission onto layers 2/3 and 5/6 pyramidal cells. (A) Representative sEPSC traces recorded from layer 2/3 principal neurons in WT and C1qa KO mice, voltage-clamped at −65 mV (right) (WT: n = 5 cells, n = 3 mice; KO: n = 5 cells, n = 4 mice). **(B)** C1qa KO mice show an increase of sEPSC amplitude. **(C)** sEPSC frequency and **(D)** sEPSC decay time constant are unaltered in comparison with aged-matched control group. **(E)** sEPSC rise time is decreased in the KO group. **(F)** Representative sEPSC traces recorded from layer 5/6 principal neurons in WT and C1qa KO mice, voltage-clamped at −65 mV (right) (WT: n = 5–6 cells, n = 5 mice; KO: n = 14–16 cells, n = 8 mice). **(G)** C1qa KO mice show an increase of sEPSC amplitude and **(H)** sEPSC frequency. **(I)** sEPSC decay time constant and **(J)** sEPSC rise time unaltered in comparison with aged-matched control group. **(K)** sIPSC recordings from layer 2/3 pyramidal cells in C1qa KO and aged-matched WT mice. Neurons were voltage-clamped at 0 mV (right) (WT: n = 6 cells, n = 4 mice; KO: n = 7 cells, n = 5 mice). C1qa KO mice did not show any changes in **(L)** sIPSC amplitude, **(M)** sIPSC frequency, **(N)** sIPSC decay time constant and **(O)** sEPSC rise time. **(P)** sIPSC recordings from layer 5/6 pyramidal cells in C1qa KO and aged-matched WT mice. Neurons were voltage-clamped at 0 mV (right) (WT: n = 14–15 cells, n = 5 mice; KO: n = 24 cells, n = 8 mice). C1qa KO mice did not show any changes in **(Q)** sIPSC amplitude, **(R)** sIPSC frequency, **(S)** sIPSC decay time constant and **(T)** sEPSC rise time. Data presented as mean ± SEM; *p < 0.05, two-tailed unpaired *t* test.

We next measured mouse spontaneous exploration, locomotion, and anxiety-like-behaviors, by using Open Field testing (Kraeuter et al., 2019) (Fig. 5B, F-H, Table S6). We did not find any significant differences between C1qa KO and WT mice for measures of time spent in center area of the arena (Fig. 5F) and total distance travelled (Fig. 5G). No locomotor activity changes were found between groups during a 20-min exploration of open field arena; both KO and WT groups exhibited increased distance travelled along borders in comparison to center area (Table S6), and velocity was similar between groups (Table S6). Taken together, these results indicate that C1q deficiency does not affect general locomotor activity or spontaneous exploration behavior in the open field. However, the enhanced aversive response to the light zone in the light/dark box suggests that C1qa KO mice exhibit a context-dependent anxiogenic phenotype.

In addition, to assess compulsive-like behaviors, we employed the marble burying test, where increased burying is typically interpreted as perseverative behavior (Thomas et al., 2009), whereas normal levels of burying are considered to reflect a natural, species-typical behavior (Samalens et al., 2025). C1qa KO mice did not differ significantly from age-matched WT controls in the number of marbles buried (Fig. S3A and S3B, Table S6), reinforcing that their altered behavioral phenotype does not extend to repetitive marble digging.

Social behavior was quantified using the three-chamber social interaction test (Fig. 5I-L, Table S6), which measures sociability (preference for a social over a non-social environment) and social novelty (preference for a novel conspecific over a familiar one) (Jabarin et al., 2022). Both WT and C1qa KO mice exhibited typical sociability, spending significantly more time interacting with the novel mouse (Stranger 1- S1) than the empty cup. C1qa KO mice also spent more time exploring the empty cup compared to WT mice (Fig. 5I-K). In the social novelty phase, no significant differences were observed between genotypes in preference for the novel (Stranger 2) versus familiar (Stranger 1) mouse, indicating that both groups displayed similar social novelty recognition (Fig. 5L). Despite previous studies showing no significant changes in social interaction during a 5-minute test in C1qa-deficient mice (Madeshiya et al., 2022), our results reveal a subtle, context-dependent deficit in social behavior in a 10-minute test.

Finally, we assessed short-term escape-oriented and depressive-like immobility behaviors using the Tail Suspension Test, the most widely employed paradigm for evaluating depressive-like and antidepressant-related phenotypes in genetically modified mice (Cryan et al., 2005). We found that C1qa KO mice spent less time immobile during the 6-minute test (Fig. S4A and S4B, Table S6), indicating that C1qa deficiency contributes to enhanced stress-induced response (Madeshiya et al., 2022).

2.5. MGE-derived Interneurons successfully integrate into WT and C1qa KO cortical circuits

To first confirm integration of MGE-derived interneurons prior to evaluating their therapeutic efficacy in C1qa-associated comorbidities (Fig. 7A), we assessed migration, differentiation, and synaptic connectivity 60 days after bilateral MGE progenitor cell injection at postnatal day 2 (Fig. 6). As previously reported (Alvarez-Dolado et al., 2006; Howard and Baraban, 2016; Paterno et al., 2024), transplanted cells dispersed extensively, up to ~2000 μm from the injection site, and were distributed across cortical subregions (Figs. 6A and 6B, Fig. S5, Table S7; Video S1). These cells differentiated into PV- and SST-expressing interneurons (Figs. 6D and 6E) and received both excitatory and inhibitory synaptic inputs from host cortical pyramidal neurons (Fig. 6F), indicating successful integration into local circuits. Importantly, we observed no major differences in migration or subtype specification between WT and C1qa KO recipients (Table S7), except for less PV-INs at −1800 μm from the injection site in KO mice. The total number of PV-INs and SST-INs were similar in KO and WT mice (Fig. 6C, Table S7). These findings suggest that even a pathological cortical network does not impair the developmental trajectory of transplanted MGE-derived cells (Fig. 6B and S5A).

2.6. Interneuron transplantation insufficiently abolished absence seizures but mitigated behavioral deficits in C1qa KO mice

Given the open question of whether comorbidities in C1qa-deficient mice are driven by reduced SST-IN density or broader synaptic dysfunction linked to C1qa loss, we tested whether transplantation of embryonic MGE progenitors could mitigate the epilepsy phenotype as has been shown for acquired forms of epilepsy (Casalia et al., 2017; Hunt and Baraban, 2015; Hunt et al., 2013).

To evaluate the potential therapeutic efficacy of interneuron transplantation (Fig. 7), we performed *in vivo* electrophysiological recordings in transplanted C1qa KO and WT mice (and their respective *sham* control groups) at 67 DAT. Transplanted KO mice showed approximately 32 %, 27 % and 39 % reduction in SWDs frequency, mean duration, and percentage time spent seizing, respectively (Fig. 7B, Table S1). Transplanted or sham WT mice do not display SWD activity. While the reduction in the absence epilepsy phenotype was modest, ethosuximide-treated KO mice demonstrated a more pronounced improvement in seizure activity parameters (Fig. 1E). These findings suggest that MGE transplantation does not sufficiently rescue the absence epilepsy phenotype in C1qa-deficient mice, indicating that core circuit deficits driving SWDs persist despite the integration of MGE-derived interneurons into cortex.

In a separate cohort, we evaluated behavior, focusing on assays where C1qa KO mice had previously exhibited pronounced alterations including dark light test (Fig. 7C-D), tNORT (Fig. 7E-M) and three chamber test (Fig. S7). In the dark–light test, C1qa KO sham mice spent less time in the light zone, resembling the behavior of naive C1qa KO mice (Figs. 7C and 7D). Notably, transplantation at 60 DAT increased time spent in the light zone in C1qa KO mice to WT levels, without altering the number of transitions between chambers, demonstrating a clear rescue of the dark/light preference impairment (Figs. 7C and 7D, Table S8).

To re-assess somatosensory cortex–dependent behavior after MGE transplantation, we performed the tNORT in transplanted (Fig. 7) and sham-treated mice (Fig. 7, Fig. S6). MGE transplantation abolished the whisker-dependent discrimination impairment previously observed in C1qa KO mice, with no significant differences in discrimination ratio between transplanted WT and C1qa KO mice (Fig. 7F, G) and similar

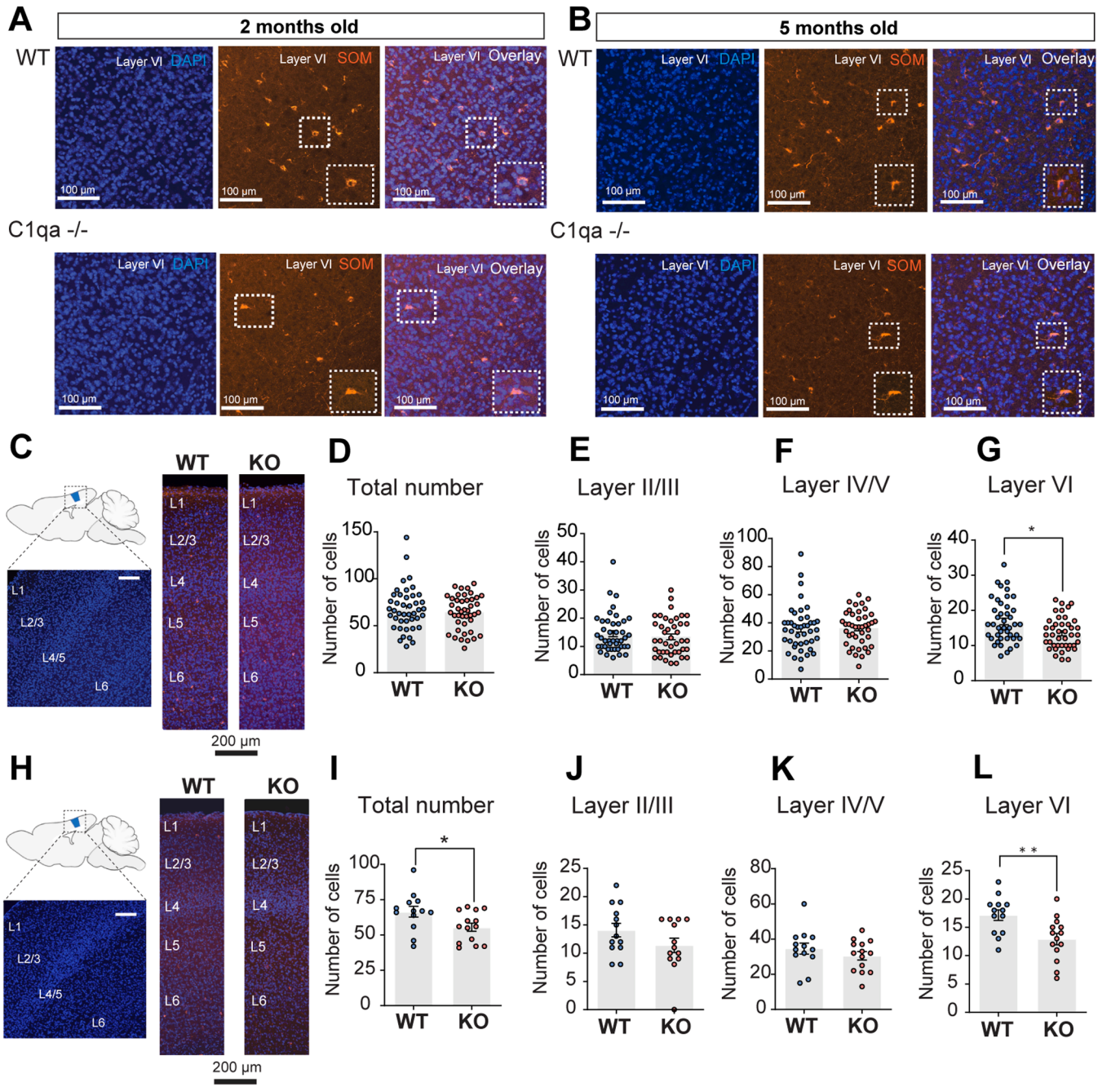

Fig. 3. Selective reduction of SST-expressing interneurons in layer VI of somatosensory cortex. (A, B) Representative images of SST-immunostained sections from WT and C1qa KO mice at 2 and 5 months of age, respectively. **(C)** Schematic of cortical layers in primary somatosensory cortex (S1) at two months old. **(D)** At 2 months of age, quantification of SST-IN density showed no significant difference in the total number of SST-INs (WT: n = 43 slices from 9 mice, KO: n = 42 slices from 8 mice; unpaired two-tailed t test), **(E)** layer II/III, or layer IV/V **(F)**. However, a significant reduction was observed in layer VI SST-INs in C1qa KO mice **(G)**. **(H)** Schematic of cortical layers in primary somatosensory cortex (S1) at five months old. **(I)** There was a significant difference in total SST-IN count (WT: n = 13 slices from 3 mice, KO: n = 12–14 slices from 3 mice). **(J)** Layer II/III, and **(K)** layer IV/V did not show any significant differences between WT and KO. **(L)** A significant reduction persisted in layer VI of KO mice ($p = 0.0056$). Data presented as mean ± SEM; *$p < 0.05$, unpaired two-tailed t test.

total exploration time within objects across training and testing sessions (Fig. 7J, K). Neither preference index (Fig. 7H-I) nor the number of exploration (Fig. 7L-M) differed significantly across groups. These findings suggest that MGE transplantation restores cortical inhibitory function in C1qa KO mice, selectively improving whisker-guided exploration (Table S9).

Given the previously observed deficit in social preference in C1qa KO mice, we next performed the three-chamber test (Fig. S7, Table S10). Transplanted C1qa KO mice exhibited sociability and social novelty indices comparable to transplanted WT controls. No differences were detected between sham WT and KO groups. These results show that MGE transplantation also rescued the sociability deficit previously reported in naive C1qa KO mice. Social novelty preference did not differ across groups (Fig. S7, Table S10).

3. Discussion

Disturbances in physiological processes during development can critically reshape circuit dynamics and contribute to both the emergence and progression of epilepsy (Cavazos and Cross, 2006). Our study

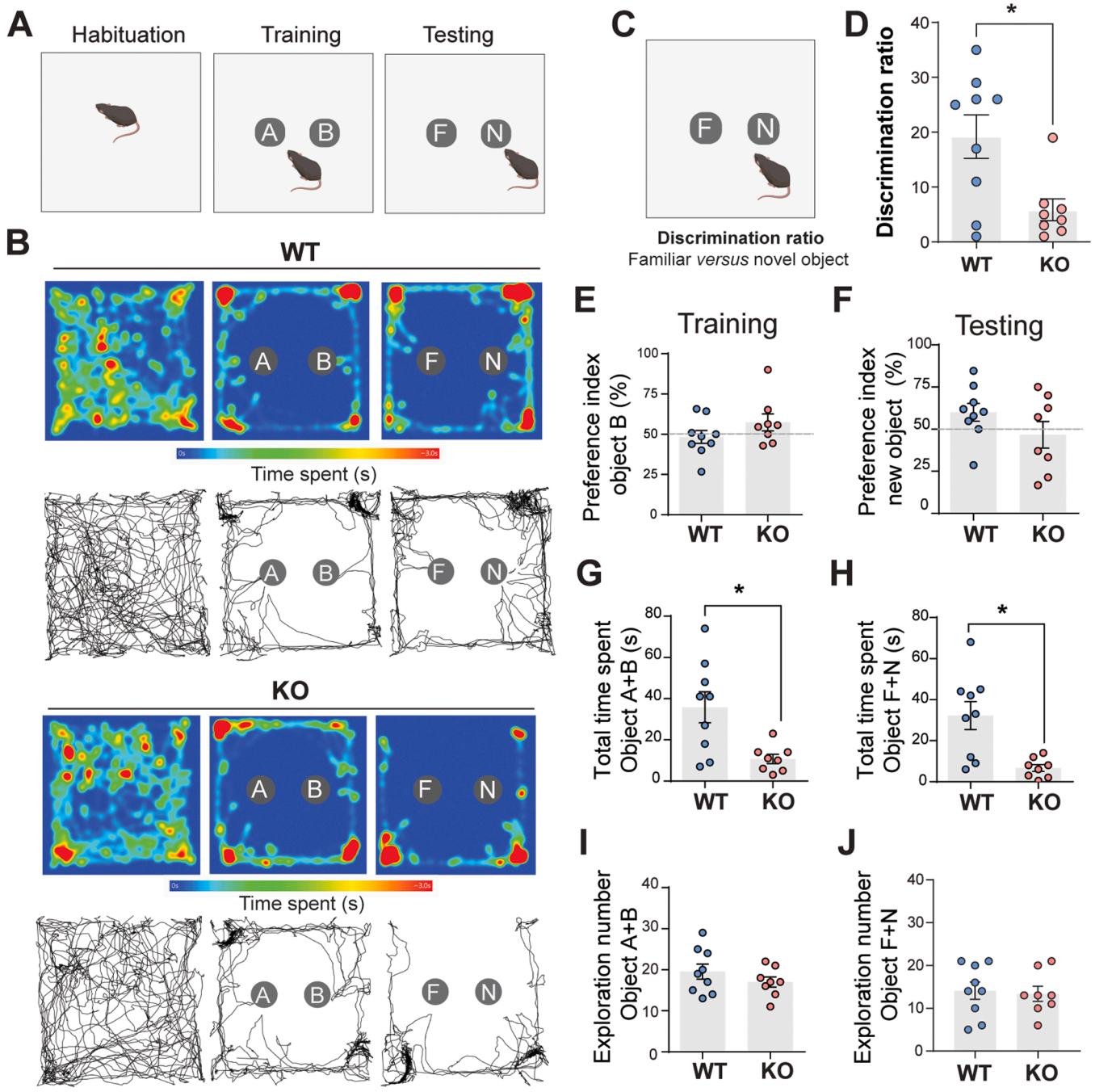

Fig. 4. Impaired texture discrimination and reduced whisker-mediated exploratory behavior in the textured novel object recognition test (tNORT). (A) Schematic of the tNORT paradigm and timeline. **(B)** Representative heatmaps of time spent exploring objects, and the locomotion track during the test. **(C-D)** During the testing session, C1qa KO mice showed a significantly lower discrimination index (DI) compared to WT controls, indicating impaired textured object recognition (WT: n = 9 mice, KO: n = 8 mice). **(E–F)** No significant differences in preference index (PI) were observed during either the training or testing sessions. **(G–H)** KO mice spent significantly less total time exploring the objects during both training and testing phases (*$p < 0.05$). **(I–J)** The number of exploratory events did not differ significantly between genotypes. Data presented as mean ± SEM; *$p < 0.05$, unpaired two-tailed t test.

addresses how loss of the complement component C1qa, a key mediator of synaptic pruning during postnatal development, impact long-term synaptic, functional, and behavioral features in C1qa KO mice. We show that germline deletion of C1qa in mice results in electrographic spike-and-wave discharges (Fig. 1), cortical hyperexcitability (Fig. 2), reduction of layer 6 SST-expressing interneurons (Fig. 3), impaired sensory-driven exploration (Fig. 4), and context-dependent behavioral alterations (Fig. 5).

While insufficient and/or aberrant complement-dependent synaptic pruning, particularly at excitatory synapses, has been implicated in epileptogenic processes (Chu et al., 2010; Holden et al., 2021; Stevens et al., 2007; Whitelaw, 2018), the potential pruning of inhibitory synapses remains largely unexplored. Although studies have shown that complement activation can drive microglial pruning of inhibitory synapses, leading to network hyperexcitability and contributing to both abnormal behaviors (Lui et al., 2016), epilepsy (Fan et al., 2023) and Alzheimer's disease (Dejanovic et al., 2022), these findings offer limited insight into whether interneuron subtypes are preferentially targeted or how complement cascade dysregulation disrupts inhibitory network remodeling at the cellular level and drives circuit instability that

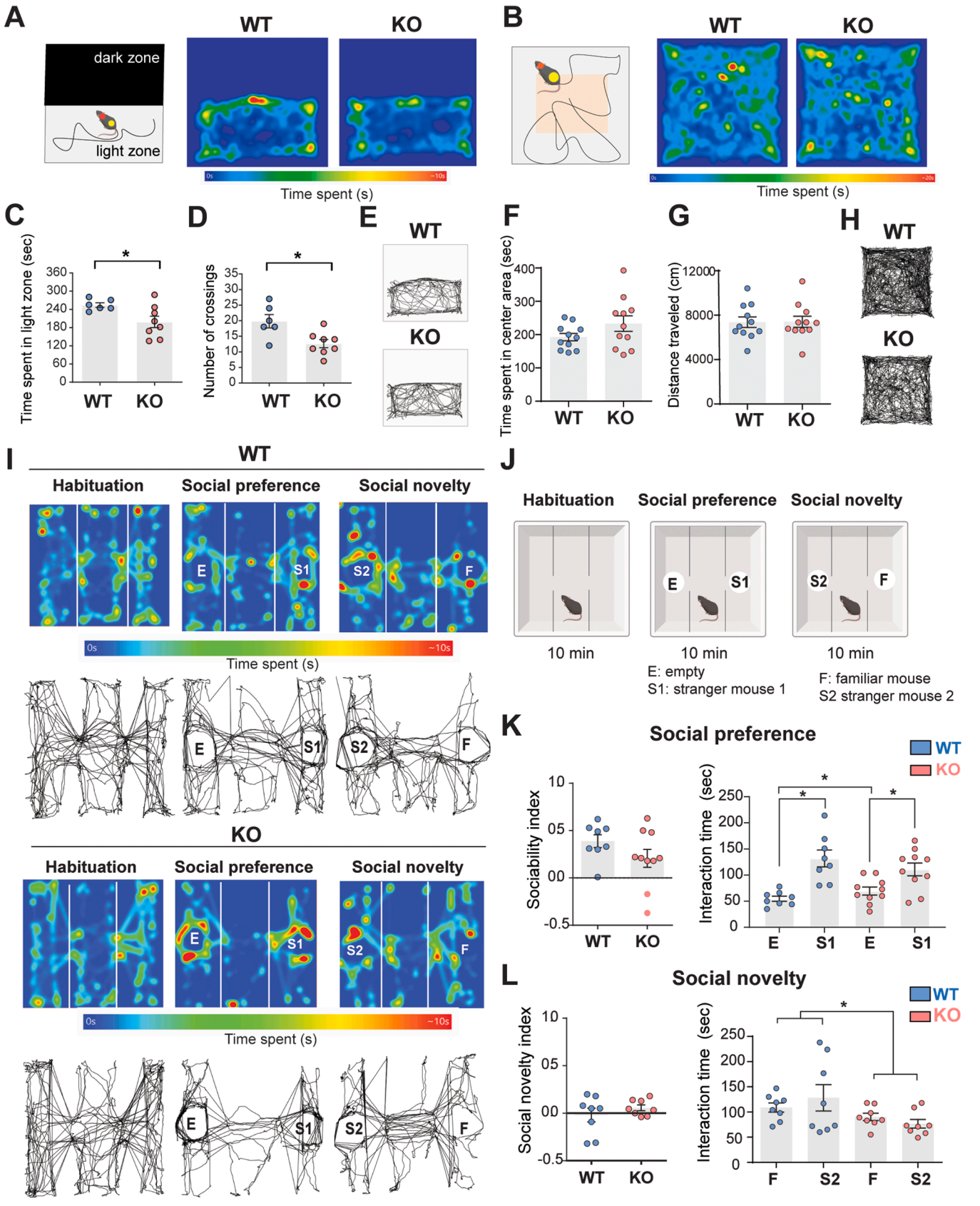

(caption on next page)

Fig. 5. Context-specific anxiety-like behavior in the light/dark test but normal exploration and locomotion in open field. (A-B) Schematic of the light/dark test setup and open field test, followed by heat map of time spent in the apparatus. **(C)** C1qa KO mice spent significantly less time in the light zone compared to WT controls, indicating increased anxiety-like behavior. **(D)** KO mice also exhibited fewer transitions between light and dark chambers (WT: n = 6 mice, KO: n = 8 mice, *p < 0.05, unpaired two-tailed t test). **(E)** Trajectory plot locomotion patterns illustrate similar locomotor profiles across groups. **(F–G)** No significant differences were found between C1qa KO and WT mice in time spent in the center zone or total distance travelled during open field test, indicating intact exploratory behavior (WT: n = 11 mice, KO: n = 11 mice, (p > 0.05, unpaired two-tailed t test). **(H)** Locomotor trajectory plot illustrates similar locomotor profiles across groups. **(I–L)** Social behavior was assessed using the three-chamber social interaction test. **(J-K)** During the sociability phase, both WT and C1qa KO mice showed a preference for interacting with a novel conspecific (Stranger 1, S1) over the empty cup, and KO mice spent more time exploring the empty cup than WT mice (WT: n = 8 mice, KO: n = 10 mice). **(L)** C1qa KO and WT did not show any significant alteration in social novelty (WT: n = 8 mice, KO: n = 8 mice, p > 0.05). Data presented as mean ± SEM; * p < 0.05, Two-way ANOVA, Tukey's multiple comparisons test.

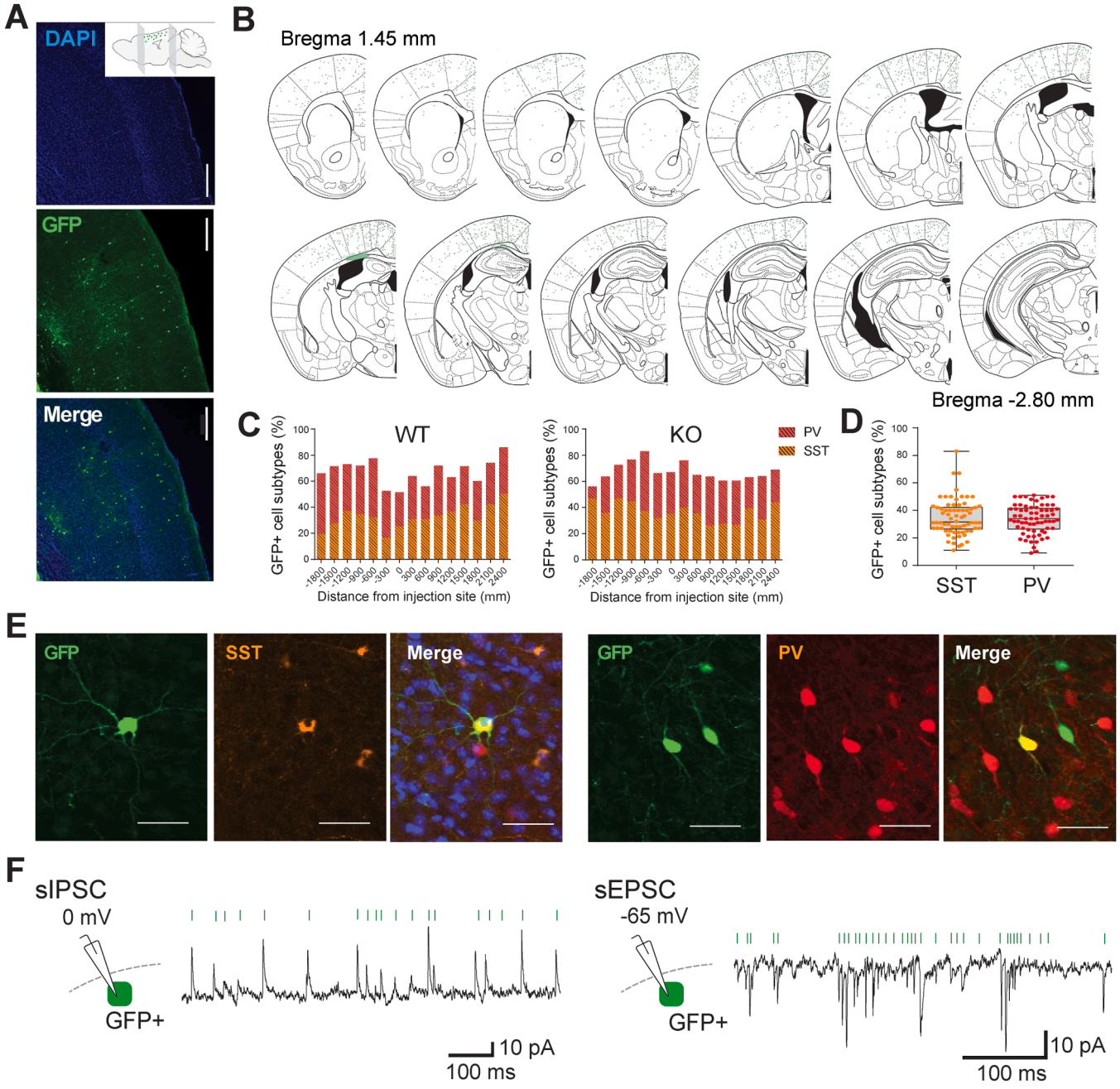

Fig. 6. Transplanted MGE progenitors migrate and differentiate into mature interneurons. (A) Immunofluorescence image of somatosensory cortex at 60 days after transplantation (DAT) showing GFP⁺ cells derived from MGE progenitors (WT: 12–16 slices /mice, 2 mice; KO: 14–15 slices per mice, 3 mice). **(B)** Schematic representation of GFP⁺ cell distribution across cortical layers in wild-type (WT) mice. **(C)** Quantification of interneuron subtypes reveals similar distribution across cortex. **(D)** Bar graph showing the proportion of GFP⁺ cells expressing PV or SST (WT: n = 2 mice, KO: n = 3 mice). **(E)** Confocal images showing co-labeling of GFP⁺ cells with PV and SST antibodies. Data presented as mean ± SEM; unpaired t test (WT *vs* KO). **(F)** Whole-cell patch-clamp recordings from GFP⁺ cells showing spontaneous inhibitory postsynaptic currents (sIPSCs, left) and excitatory postsynaptic currents (sEPSCs, right).

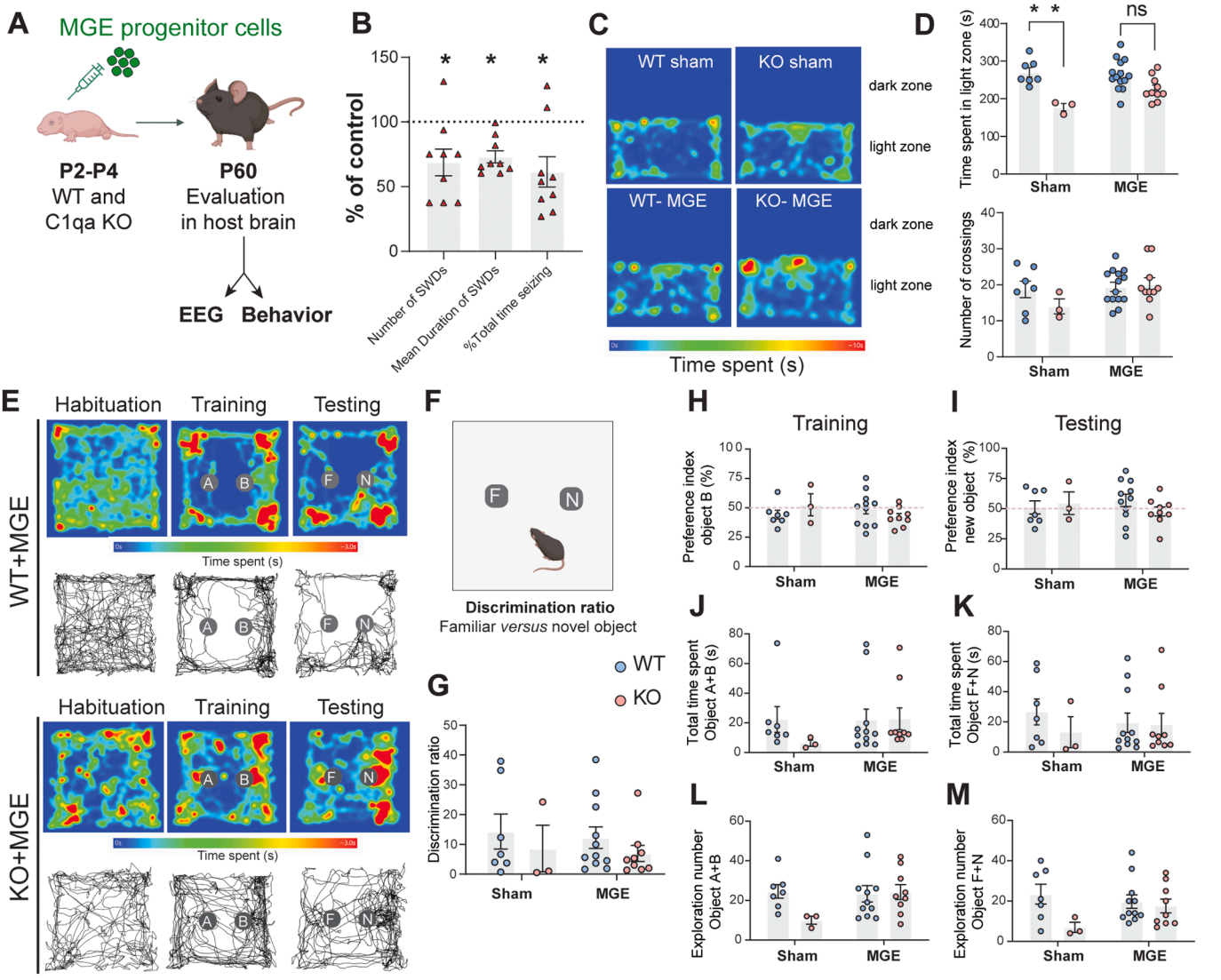

Fig. 7. Transplantation of MGE progenitors reduce SWDs and improve behavioral performance. (A) Experimental timeline for behavioral and electrophysiological assessments following MGE transplantation. **(B)** Quantification of SWDs expressed as a percentage relative to genotype-matched control mice (KO sham: n = 2 male mice, KO transplanted: n = 4 male mice). **(C)** Heat map showing time spent in the light zone during the dark–light box test. **(D)** Quantification of time spent in the light chamber (top) and number of crossings (bottom) (WT: n = 7 mice [3 females, 4 males], WT transplanted: n = 14 mice [6 females, 8 males]; KO: n = 3 mice [3 males], KO transplanted: n = 10 mice [6 females, 4 males], two-way ANOVA, *p < 0.05). **(E)** Heat map showing time spent near objects and exploration trajectory during the tNORT test (WT: n = 7 mice [4 females, 3 males], WT transplanted: n = 11 mice [7 females, 4 males]; KO: n = 3 mice [3 males], KO transplanted: n = 9 mice [7 females, 2 males], two-way ANOVA, *p < 0.05). **(F)** Schematic of the discrimination ratio apparatus used during the test session followed by **(G)** Discrimination ratio across groups (sham vs. transplanted; WT and KO). **(H–I)** Preference index during the training and testing sessions, respectively. **(J–K)** Total time spent exploring both objects during training and testing sessions. **(L–M)** Number of exploratory interactions with each object during training and testing sessions, respectively. Data presented as mean ± SEM; *$p < 0.05$.

manifests as network-level functional abnormalities. To our knowledge, this is the first study to directly characterize inhibitory neuron subtype-specific changes and long-term functional effects of germline C1qa deletion in mice.

Interneurons are crucial for maintaining inhibitory tone and for shaping excitatory activity across cortical circuits (Calcagnotto, 2016; Righes Marafiga et al., 2021). Although the mechanisms by which C1q loss leads to a reduction of SST interneurons remain unclear, interneuron loss has been associated with the development of recurrent spontaneous seizures (Cobos et al., 2005; Dinocourt et al., 2003; Huusko et al., 2015; Kobayashi and Buckmaster, 2003; Rossignol et al., 2013). In the present study, we found that C1qa KO mice exhibited increased excitatory input onto L2/3 and L5/6 pyramidal neurons in the somatosensory cortex, while L2/3 and L5/6 inhibitory synaptic transmission remained unchanged. Because the reduced number of SST-expressing interneurons in layer 6 did not compromise lateral inhibition onto local pyramidal neurons from deep layers, or distal dendritic inhibition in superficial layers of the somatosensory cortex (Ramaswamy et al., 2017; Silberberg and Markram, 2007), we suggest that changes in inhibitory neuron density alone are unlikely to account for the enhanced excitatory drive onto cortical pyramidal cells. Consistent with this, previous studies have shown that germline deletion of C1qa during early development is associated with enhanced excitatory transmission and connectivity abnormalities, without affecting inhibitory synaptic transmission (Chu et al., 2010). The underlying mechanisms appear to involve an increased density of axonal boutons in deep cortical layers, as well as structural modifications of layer 5 basal dendrites, as previously described (Ma et al., 2013). Future studies will be essential to determine whether reduced SST-INs numbers are accompanied by intrinsic, structural and synaptic deficits that contribute to

cortical network dysregulation in C1qa-deficient mice.

To date, in both human patients and animal models of epilepsy, elevated C1qa expression also has been found to correlate with impaired excitatory synaptic transmission and the emergence of epileptic spindles (Holden et al., 2021), seizure frequency and progression (Aronica et al., 2007; Schartz et al., 2018; Wyatt et al., 2017), implicating excessive complement activation in increased seizure susceptibility. Altogether, these findings underscore a dual and context-dependent role for C1qa in epileptogenic processes, wherein both hyperactivation and deficiency of the complement cascade can destabilize neural networks and contribute to neurological disorders and comorbidities (Schartz and Tenner, 2020; Schartz et al., 2018; Sierra et al., 2022; Wyatt et al., 2017).

Dysregulation of the classical complement cascade has been implicated in neuroinflammatory and degenerative processes across various neurological disorders (Carvalho et al., 2019; Dejanovic et al., 2022; Lui et al., 2016; Madeshiya et al., 2022), raising the possibility that seizure generation may also occur through mechanisms independent of C1qa loss. Indeed, in humans, C1q deficiency is not a primary cause of seizures; however, approximately 67 % of patients with systemic lupus erythematosus (SLE) experience seizures through mechanisms that remain poorly understood (van Schaarenburg et al., 2016). In addition to C1q, complement component C3 has been implicated in pathological processes contributing to aberrant synaptic pruning (Gomez-Arboledas et al., 2021) and neurodegeneration (Jiang et al., 2021; Wei et al., 2021). Astrocyte-derived C3 has been shown to mediate synaptic damage and is markedly upregulated following *status epilepticus* (Wei et al., 2021). Nonetheless, recent studies implicate microglia as critical mediators of inhibitory synapse elimination in temporal lobe epilepsy (TLE), primarily through complement C3–C3aR–dependent engulfment of inhibitory synapses (Chen et al., 2025). This mechanism likely contributes to network hyperexcitability and interneuron loss, highlighting a pathway by which complement signaling may facilitate seizure generation.

Because aberrant activation of the complement cascade, particularly C1q, could potentially exacerbate neuroinflammation or synaptic loss (Hong et al., 2016; Wilton et al., 2023), we instead pursued a strategy focused on the transplantation of inhibitory neurons derived from the medial ganglionic eminence (MGE). Specifically, we hypothesized that interneuronal deficit plays a critical role in the enhanced excitability and seizure activity observed in C1qa KO mice, a mechanism distinct from the excitatory synaptic changes previously described. Advances in cell-based transplantation therapies offer the potential for neuron subtype-specific interventions, such as transplantation of MGE interneuron progenitors, which have shown efficacy across a range of epilepsy syndromes, as supported by multiple prior studies (Baraban et al., 2009; Calcagnotto et al., 2010a; Hunt et al., 2013; Wang et al., 2025; Zipancic et al., 2010). This approach has the potential to enhance or re-establish the inhibitory circuitry within pathological networks (Alvarez-Dolado et al., 2006; Calcagnotto et al., 2010b), as transplanted MGE-derived interneurons integrate into host cortical circuits (Fig. 6) and mitigate both behavioral comorbidities and seizure burden (Alvarez-Dolado et al., 2006; Baraban et al., 2009; Calcagnotto et al., 2010b; Casalia et al., 2017; Howard and Baraban, 2016; Hsieh and Baraban, 2017; Zipancic et al., 2010).

Our results show that interneuron transplantation had a robust rescue effect on behavioral comorbidities, including dark light preference task and sensory-driven exploratory behavior, but did not effectively treat the absence epilepsy phenotype (Fig. 7). Given that early transplantation (e.g. P1-P4) results in widespread cell migration and integration (Fig. 6, Video V1) (Hsieh and Baraban, 2017; Paterno et al., 2024), we speculate that the observed rescue in specific behaviors (Fig. 7), such as performance in the light/dark box, may reflect broader network reorganization in regions not directly assessed by our molecular or electrophysiological analyses. Importantly, prior studies have shown that transplantation of MGE cells into wild-type mice does not present untoward side effects (Alvarez-Dolado et al., 2006; Howard and Baraban, 2016; Hsieh and Baraban, 2017; Paterno et al., 2024), supporting the overall safety of this intervention and suggesting that broader circuit integration may be beneficial rather than detrimental. In the present study, wild-type and KO mice display similar cortical migration and integration of MGE-derived interneurons (Fig. 5). Notably, rescue of whisker-dependent exploratory behavior after transplantation (Fig. 7) suggests that impaired SST-mediated inhibition within somatosensory cortex contributes to deficits in sensory processing observed in C1qa KO mice.

In contrast, MGE transplantation did not abolish spike-and-wave discharges in the EEG, demonstrating limited efficacy comparable to ethosuximide (Fig. 7). Although absence seizures are traditionally linked to corticothalamic circuit dysfunction (Crunelli and Leresche, 2002), our strategy focused on MGE transplantation in cortex under the hypothesis that enhancement/restoration of inhibitory circuitry would be sufficient to reduce thalamo-cortical spike-and-wave activity. However, unlike other epilepsy models where MGE transplantation reduces seizures by 88–92 % compared to non-transplanted controls (Casalia et al., 2017; Hunt et al., 2013), this approach failed to achieve dramatic seizure reduction in C1qa KO mice. These findings suggest that while cortical interneuron dysfunction contributes to absence-like seizures in C1qa KO mice, additional mechanisms and brain regions are likely involved. In this context, GABAergic synaptic interactions between cortical and thalamic networks may constitute a central network hub in the generation of SWDs (Lindquist et al., 2023). Evidence indicates that elevated C1q in the thalamus disrupts synaptic transmission, drives neuronal loss and neuroinflammation, and is linked to pathological network activity, including epileptic spikes and sleep spindle disruption (Holden et al., 2021), suggesting that alterations in the complement cascade could compromise thalamic interneurons. Although we did not directly examine these interneurons or the thalamic network, such deficits may contribute to absence-like seizure generation and could help explain the insufficient seizure phenotype rescue observed following cortical interneuron transplantation.

Therefore, our findings lead to two main conclusions: (1) downregulation of C1qa in mice induces synaptic, functional, and behavioral abnormalities that persist into adulthood; and (2) dysfunction of inhibitory circuitry alone is insufficient to account for the full spectrum of comorbidities observed in C1qa KO mice.

This study establishes that C1qa downregulation causes enduring circuit and behavioral abnormalities, highlighting the complement system as an important modulator of brain function in health and disease (Presumey et al., 2017; Schartz and Tenner, 2020; Schulz and Trendelenburg, 2022; Stevens et al., 2007; Tenner et al., 2018; Zhang et al., 2023). This is a critical area of discussion, as fine-tuned regulation of the complement pathway may drive region- and circuit-specific changes in the brain. Future studies are needed to define the threshold at which complement cascade modulation shifts from beneficial to deleterious in neurological disorders.

3.1. *Limitations of the study*

This study provides an inhibitory network perspective in a model previously understood mainly through its excitatory contributions to spike-and-wave discharges. The identification of long-term alterations in inhibitory neuron density may represent the first step toward investigating how sustained changes in inhibitory networks contribute to ictogenesis. We analyzed SST- and PV-interneuron densities in the somatosensory cortex and evaluated their functional consequences in this mouse model of absence epilepsy. Further characterization of SST-INs function and integration, as well as structural analyses of inhibitory and excitatory synapses, could strengthen our understanding of inhibitory–excitatory dynamics in seizure generation and should be addressed in future studies.

Dissecting the causal mechanisms underlying genetic epilepsies and their behavioral comorbidities remains challenging, as it is often

difficult to determine whether comorbid disturbances arise independently of seizures. In this study, interneuron transplantation ameliorated behavioral comorbidities and partially rescued the seizure phenotype, indicating that these outcomes are not fully interdependent. We note that some behaviors, such as anxiety-like behavior, could potentially interfere with the interpretation of other behavioral tests, representing an inherent limitation of the model that cannot be fully mitigated.

Importantly, an interplay of excitatory and inhibitory circuit dysfunctions across multiple neuronal populations, as well as consequences of C1q loss and downstream complement pathway alterations, may contribute to the phenotype and warrant further characterization. Collectively, these results highlight epileptic disorders as multifaceted network diseases, in which circuit-level dysfunction drives pathology and underscores the need for multi-targeted therapeutic strategies.

4. Material and methods

4.1. Animals and ethics

All protocols and procedures were in accordance with the guidelines of the Laboratory Animal Resource Center at the University of California, San Francisco (IACUC; protocol #AN208171–00). Experiments were performed on young adult (2-month-old) and mature adult (5-month-old) male C1qa knockout (KO; −/−, strain #031675) mice and their age-matched wild-type (WT; C57BL/6 J) controls, all purchased from The Jackson Laboratory (US). For transplantation of MGE-derived interneurons, P1–P4 mice served as recipients. GFP+ embryos were obtained from β-actin:GFP mice (Jackson Laboratory, strain #006567). Male mice were used for *in vitro* and *in vivo* electrophysiological recordings and behavioral assays. Mixed-sex cohorts were used exclusively for behavioral experiments following transplantation, as will be indicated in the figure captions. Animals were housed in a 12 h dark/light cycle, temperature- and humidity-controlled environment with water and food ad libitum. All tests were conducted in the light cycle. In all experiments, animals were habituated to the testing room 30 min before the tests. The genotypes of all mice were determined by real time PCR (Transnetyx, Cordova, TN) with specific probes designed for each gene. A schematic overview of the study design, including electrophysiology, behavioral testing, immunostaining, and MGE progenitor cell transplantation is shown in Figure S8.

4.2. In vivo electrophysiology

4.2.1. Video-electroencephalogram recordings and analysis

Electroencephalographic (EEG) recordings were obtained using a time–locked video digital EEG monitoring system (Pinnacle Technologies). Mice were weighed and anesthetized using a single intraperitoneal (i.p.) injection of ketamine and xylazine (10 mg/kg and 1 mg/kg i.p.). When no limb–withdrawal response to a noxious foot pinch was observed, each mouse was surgically implanted with electrodes placed over the frontoparietal cortex. Sterile, stainless steel bone screw recording electrodes were placed epidurally through burr holes in the skull (one electrode on either side of the sagittal suture, approximately halfway between bregma and lambda sutures and ≈1 mm from the midline) using surface head–mount EEG hardware (Pinnacle Technologies). Electrodes were cemented in place with a fast–acting adhesive and dental acrylic. Two wires were laid on the shoulder muscles for electromyographic (EMG) recording. Animals were allowed to recover for 5–7 days before experiments were initiated. Experiments were performed at 60 days old for C1qa KO mice and WT control mice, and at 67 days old for MGE transplanted mice, corresponding to 60 days after transplantation (DAT). Spike-wave discharges were defined as high-amplitude paroxysmal EEG discharges (amplitude >3-fold background) lasting for at least 2 s, with a frequency ranging from 3 to 12 Hz, accompanied by behavioral arrest. Possible SWDs events were analyzed by two investigators blinded to treatment condition of the animals using SireniaScore software (Pinnacle). We quantified 2 epochs lasting 1 h, from different daylight periods, for KO (n = 9 mice), WT (n = 4 mice), transplanted KO (n = 4 mice), sham KO (n = 2 mice), transplanted WT (n = 2 mice) and sham WT (n = 2 mice). In a separate cohort of mice, we administrated ethosuximide (200 mg/kg, i.p., Sigma Aldrich, E7138) to C1qa deficient mice (n = 2 mice), as a control validation step to confirm that the spike-and-wave discharges (SWDs) we analyzed were drug-sensitive and correctly identified.

4.3. In vitro electrophysiology

4.3.1. Slice preparation

Mice were deeply anesthetized by intraperitoneal injection of a mixture of xylazine and ketamine (concentration), and then transcardially perfused (~2 min) with an ice-cold (0–4°C) protective artificial cerebrospinal fluid containing (NMDG solution) (in mM): 93 NMDG, 2.5 KCl, 1.2 NaH2PO4, 30 NaHCO3, 20 HEPES, 25 Glucose, 5 sodium ascorbate, 3 sodium pyruvate, 10 MgSO4, 0.5 CaCl2, equilibrated with 95 % O2 / 5 % CO2.The pH of the solution was titrated to 7.3–7.4 with concentrated HCl. The brain was quickly removed and immersed into NMDG solution. Coronal 300 μM horizontal slices were prepared using a vibratome (Leica, Germany). The brain slices were recovered at 34 ± 1°C in oxygenated NMDG solution for 10 min and then transferred to oxygenated ACSF solution containing (in mM) 125 NaCl, 2.5 KCl, 1.25 NaH2PO4, 25 NaHCO3, 1 MgCl2, 25 Glucose and 2 CaCl2, pH 7.4, at room temperature. Slices were allowed to recover at least 30 min prior to all recordings.

4.3.2. Whole-cell patch-clamp recordings

Coronal slices were transferred one at a time to the recording chamber, perfused with oxygenated ACSF (32 ± 1°C) at a rate of 4 mL per min. Whole-cell recordings were obtained from visually identified neurons using an infrared differential interference contrast (IR-DIC) video-microscopy system on an upright microscope (BX51WI, Olympus). Patch electrodes (3–5 MΩ) were pulled from borosilicate glass capillary tubing (GC150TF-10, Harvard Apparatus) using a micropipette puller (DMZ Zeitz-Puller). For excitatory postsynaptic currents, intracellular solution consisted of (in mM) 140 KGluconate, 1 NaCl, 1 MgCl2, 1 CaCl2, 5 EGTA, 2 MgATP, 0.2 NaGTP, 10 HEPES, pH 7.2, 285–295 mOsm. For inhibitory postsynaptic currents, intracellular solution contained (in mM) 140 CsCl, 11 EGTA, 10 HEPES, 2 MgATP, 1 MgCl2, and 0.5 NaGTP, pH 7.25, 285–295 mOsm. Signals were digitally sampled at 10 kHz and data acquired using a MultiClamp 700B amplifier and a Digidata 1550 A. All analysis was performed using pCLAMP10 (Axon Instruments, Molecular Devices).

4.4. MGE progenitor cells dissection and transplantation

MGE progenitor cells were harvested from E13.5 GFP⁺ transgenic embryos, as previously described (Paterno et al., 2024). Cell viability was assessed using Trypan Blue (Sigma-Aldrich), and only cell preparations with > 80 % viability was used for transplantation. Pups (P1–P4) were anesthetized by brief exposure to ice until pedal reflexes were absent. Each recipient received a single injection of 5×10^4 cells into both hemispheres, using coordinates from bregma to target the cortex (1 mm anterior, 1.2 mm lateral, 0.2 mm dorsal). After bilateral cortical transplantation, pups were monitored until they fully recovered and then returned to their mothers. Post hoc analysis confirmed the presence of MGE-derived cells across cortical layers by using immunostaining. Mice in which transplantation was unsuccessful, defined by the absence of GFP⁺ transplanted cells, were excluded from further analysis. Control groups were injected with the media alone.

4.5. Immunohistochemistry

Animals were anesthetized with a mixture of Ketamine/Xylazine (i.p.) and transcardially perfused with ice-cold PBS (~3 min) followed by

50 mL of ice-cold 4 % paraformaldehyde (PFA). The brains were then removed from the skull, post-fixed (4 % PFA, 4°C, overnight), stored in PBS solution (0.1 % diazide, 4°C), and finally sliced into coronal sections (50-μm thick). Primary antibodies used: anti-GFP (Aves Labs; GFP-1020; 1:000), anti-parvalbumin (Swant Cat; #PV27; 1:1000), and anti-somatostatin (Santa Cruz Biotech, 55565; 1:200). Secondary antibodies used: Alexa 488, Alexa 647, and Alexa 594 (Invitrogen; A11039; A21244; A11005; 1:1000).

4.6. Cell counting and quantification

All images were acquired using high-resolution fluorescence microscopy (Nikon confocal microscope) under consistent acquisition settings (1024 × 1024 pixels; 4 × and 10 × objectives) and analyzed using ImageJ (NIH) and Nikon Elements Viewer. To quantify endogenous PV and SST interneurons, cell counting was restricted to anatomically matched 50 μm fluorescent sections of the somatosensory cortex, with layer-specific analysis based on established cytoarchitectural features (such as the density of cells). For transplanted MGE-derived cells analysis, we counted the number of GFP+ cells in every 6-coronal section (spaced 300 μm apart) along the rostro-caudal axis, to capture the full distribution of transplanted cells (Paterno et al., 2024). Manual counts were performed blinded to experimental condition to minimize bias.

4.7. Behavioral tests

Mice were randomly assigned to behavioral testing groups, with age-matching between groups ensured, and all experiments were conducted during the light phase under consistent environmental conditions. Most behavioral tests were conducted individually to prevent behavioral interference. Exceptions, including the Open Field, Dark-Light Preference, and Tail Suspension tests, were performed with overlapping cohorts to minimize the total number of animals used (Figure S8). All mice were included in the analysis, except in cases where technical or methodological factors prevented inclusion. Transplanted mice underwent the same behavioral battery, with 5–7-day intervals between assays to minimize stress and potential carryover effects.

4.7.1. Open field test

Mice were placed in the center of a square arena (40 × 40 cm^2) with opaque gray walls and allowed to explore freely for 20 min while being video recorded. The arena was divided into central (20 × 20 cm^2) and peripheral (20 cm wide) zones for analysis. Distance traveled, velocity, and time spent in each zone were quantified using EthoVision (Noldus Information Technology).

4.7.2. Dark/Light box

Mice were placed in the light compartment of a light/dark box, and behavior was recorded for 10 min. Time spent in each chamber and the number of light/dark transitions were quantified. Illumination was kept constant in the light chamber, while the dark chamber was enclosed with black paper to block external light.

4.7.3. Tail suspension test

Mice were suspended by the tail using adhesive tape placed < 1 cm from the tip and hung 60 cm above the chamber floor for 6 min. The test apparatus consisted of opaque white acrylic walls (20 × 40 × 60 cm) with one open side for video recording. Total immobility duration was quantified using DBscorer software (Nandi et al., 2021).

4.7.4. Marble burying test

Mice were placed in transparent cages containing ~4.5 cm of fine sawdust and 12 glass marbles arranged in a 4 × 3 grid. After 30 min, the number of marbles buried (≥ two-thirds covered by substrate) was quantified to assess anxiety- and compulsive-like behavior.

4.7.5. Three chamber sociability test

The test consisted of three sessions, lasting 10-min each, within a three-chambered box with openings between the chambers. In the first session, mice were allowed to habituate to the arena and to explore the three chambers. In the second session, a never-before met C57BL/6 J male mouse (named stranger 1) was placed under an inverted stainless steel pencil cup (9 cm height × 9 cm diameter solid bottom; with stainless steel bars spaced 1 cm apart) in one of the side chambers and another identical inverted empty cup was placed in the other side chamber. The position of the object mouse was altered between left and right chambers between subjects. In the third session, we added a second never-before-met C57BL/6 J male mouse (named novel), replacing the empty cup. The box and pencil cups were cleaned with 10 % ethanol between animals and before the first animal. Time spent sniffing each cup was scored by a blind investigator using video recordings. Sociability index (SI) and social novelty index (SNI) were calculated as follows:

$$\mathrm{SI} = \frac{(\textit{time exploring stranger mouse}1 - \textit{time exploring object})}{(\textit{time exploring stranger mouse}1 + \textit{time exploring object})}$$

$$\mathrm{SNI} = \frac{(\textit{time exploring novel mouse}2 - \textit{time exploring familiar mouse})}{(\textit{time exploring novel mouse}2 + \textit{time exploring familiar mouse})}$$

4.7.6. Texture novel object recognition (tNORT)

Mice were habituated to the open field arena for 20 min on two consecutive days prior to the whisker-dependent texture discrimination test. Textured objects were cylindrical (1.5 cm radius × 10 cm height), covered with 120-grit sandpaper for familiar objects and 40-grit for novel objects. On the third day, testing consisted of two sessions: (1) the training phase, during which the mouse was placed in the center of the arena to explore two identical textured objects (120 G) for 5 min; and (2) the testing phase, during which one familiar (120 G) and one novel (40 G) textured object were placed in the arena. These sessions were separated by a 5-minute rest period in the home cage. The total time spent actively investigating all objects was video recorded. Performance during the training and testing sessions was quantified using the Discrimination Index (DI) and Preference Index (PI). DI was calculated as the difference in time spent exploring novel versus familiar (or identical) objects divided by the total exploration time. PI was calculated as the time spent exploring either the familiar or novel object divided by the total exploration time, expressed as a percentage.

$$\textit{PI training} = \frac{\textit{time spent exploring object } B}{\textit{Total time exploring objects } A+B} * 100$$

$$\textit{PI testing} = \frac{\textit{time spent exploring novel object}}{\textit{Total time exploring familiar} + \textit{novel objects}} * 100$$

$$\textit{DI training} = \frac{\textit{time spent exploring object } B - \textit{time spent exploring object } A}{\textit{Total time exploring objects } A+B}$$

$$\textit{DI testing} = \frac{\textit{time spent exploring novel object} - \textit{time spent exploring familiar object}}{\textit{Total time exploring familiar} + \textit{novel objects}}$$

4.7.7. Whisker nuisance test

The Whisker Nuisance (WN) test was conducted as described by (Balasco et al., 2022a). Mice were housed individually for at least one week prior to the start of experimentation. They were habituated to their individual experimental cages for 30 min per day over three consecutive days, under constant observation by a researcher. Immediately following the final habituation session on day three, the WN test was performed. The test consisted of one 5 min sham stimulation period followed by three 5 min trials of whisker stimulation, with 1 min inter-trial intervals. Stimulation was delivered using a blunt wooden stick (20 cm length), with the researcher gently bending the middle portion of the whiskers and alternating sides of the snout approximately every 3 s. Sham stimulation was conducted using the same stick and motion without contacting the whiskers. The test was video recorded and later analyzed for the following behaviors: fearful responses, stance, breathing/hyperventilation, responsiveness, and evasiveness. Each segment of the test (sham and three stimulation trials) was blindly scored using a qualitative scale from 0 to 2 (0: absent; 1: barely present/ambivalent behavior; 2: present for most of the trial).

4.8. Tissue preservation, clearing, and Light Sheet Imaging

Two months following MGE transplantation, brain tissue was collected after cardiac perfusion with 1X PBS supplemented with heparin (10 U/mL) followed by ice-cold 4 % paraformaldehyde (PFA) (Electron Microscopy Sciences). Tissues were collected and underwent overnight fixation in 4 % PFA solution at 4 °C. Paraformaldehyde-fixed samples were preserved with SHIELD reagents (LifeCanvas Technologies) using the manufacturer's instructions (Park et al., 2018). Samples were delipidated using LifeCanvas Technologies Clear+ delipidation reagents. Following delipidation, samples were incubated in 50 % EasyIndex (RE = 1.52, LifeCanvas Technologies) overnight at 37°C followed by 1d incubation in 100 % EasyIndex for refractive index matching. After index matching the samples were imaged using a SmartSPIM axially-swept light sheet microscope using a 3.6x objective (0.2 NA) (LifeCanvas Technologies).

4.9. Statistical analysis

Comparisons between two groups (WT versus KO) were tested with unpaired two-tailed t test. One-way ANOVA was used for more than two groups' comparisons with one condition, followed by a post hoc test for multiple comparisons. Two-way ANOVA was used for more than two groups' comparisons with two or more conditions, followed by a post hoc test for multiple comparisons. The number of animals per group and statistical analysis are displayed in the figure captions and supplementary tables, respectively.

CRediT authorship contribution statement

Jessica Bowlus: Methodology, Investigation, Formal analysis. **Thy Vu:** Methodology, Investigation, Formal analysis. **Baraban Scott C:** Writing – review & editing, Writing – original draft, Resources, Conceptualization. **Joseane Righes Marafiga:** Writing – review & editing, Writing – original draft, Visualization, Validation, Supervision, Project administration, Methodology, Investigation, Funding acquisition, Formal analysis, Data curation, Conceptualization.

Funding

This work was supported by the National Institutes of Health (R01-NS071785–15 to S.C.B.).

Declaration of Competing Interest

The authors declare that they have no known competing financial interests or personal relationships that could have appeared to influence the work reported in this paper.

Acknowledgment

We would like to thank members of the Baraban laboratory (R. Paterno, C. Carpenter, P. Whyte-Fagundes & B. Zhu) for their support and constructive feedback.

Appendix A. Supporting information

Supplementary data associated with this article can be found in the online version at doi:10.1016/j.pneurobio.2026.102881.

Data Availability

The data supporting the findings of this study are available from the corresponding authors upon reasonable request.

References

Aaberg, K.M., Gunnes, N., Bakken, I.J., Lund Søraas, C., Berntsen, A., Magnus, P., Lossius, M.I., Stoltenberg, C., Chin, R., Surén, P., 2017. Incidence and prevalence of childhood epilepsy: a nationwide cohort study. Pediatrics 139.

Alvarez-Dolado, M., Calcagnotto, M.E., Karkar, K.M., Southwell, D.G., Jones-Davis, D.M., Estrada, R.C., Rubenstein, J.L., Alvarez-Buylla, A., Baraban, S.C., 2006. Cortical inhibition modified by embryonic neural precursors grafted into the postnatal brain. J. Neurosci. 26, 7380–7389.

Aronica, E., Boer, K., van Vliet, E.A., Redeker, S., Baayen, J.C., Spliet, W.G., van Rijen, P. C., Troost, D., da Silva, F.H., Wadman, W.J., Gorter, J.A., 2007. Complement activation in experimental and human temporal lobe epilepsy. Neurobiol. Dis. 26, 497–511.

Balasco, L., Chelini, G., Bozzi, Y., Provenzano, G., 2019. Whisker nuisance test: a valuable tool to assess tactile hypersensitivity in mice. Bio. Protoc. 9, e3331.

Balasco, L., Pagani, M., Pangrazzi, L., Chelini, G., Viscido, F., Chama, A.G.C., Galbusera, A., Provenzano, G., Gozzi, A., Bozzi, Y., 2022b. Somatosensory cortex hyperconnectivity and impaired whisker-dependent responses in Cntnap2. Neurobiol. Dis. 169, 105742.

Balasco, L., Pagani, M., Pangrazzi, L., Chelini, G., Ciancone Chama, A.G., Shlosman, E., Mattioni, L., Galbusera, A., Iurilli, G., Provenzano, G., Gozzi, A., Bozzi, Y., 2022a. Abnormal whisker-dependent behaviors and altered cortico-hippocampal connectivity in shank3b-/- Mice. Cereb. Cortex. 32, 3042–3056.

Baraban, S.C., Southwell, D.G., Estrada, R.C., Jones, D.L., Sebe, J.Y., Alfaro-Cervello, C., García-Verdugo, J.M., Rubenstein, J.L., Alvarez-Buylla, A., 2009. Reduction of seizures by transplantation of cortical GABAergic interneuron precursors into Kv1.1 mutant mice. Proc. Natl. Acad. Sci. USA 106, 15472–15477.

Bourin, M., Hascoët, M., 2003. The mouse light/dark box test. Eur. J. Pharm. 463, 55–65.

Calcagnotto, M.E., 2016. Interneurons: role in maintaining and restoring synaptic plasticity. Front Psychiatry 7, 86.

Calcagnotto, M.E., Zipancic, I., Piquer-Gil, M., Mello, L.E., Alvarez-Dolado, M., 2010b. Grafting of GABAergic precursors rescues deficits in hippocampal inhibition. Epilepsia 51 (3), 66–70.

Calcagnotto, M.E., Ruiz, L.P., Blanco, M.M., Santos-Junior, J.G., Valente, M.F., Patti, C., Frussa-Filho, R., Santiago, M.F., Zipancic, I., Alvarez-Dolado, M., Mello, L.E., Longo, B.M., 2010a. Effect of neuronal precursor cells derived from medial ganglionic eminence in an acute epileptic seizure model. Epilepsia 51 (3), 71–75.

Caplan, R., Siddarth, P., Stahl, L., Lanphier, E., Vona, P., Gurbani, S., Koh, S., Sankar, R., Shields, W.D., 2008. Childhood absence epilepsy: behavioral, cognitive, and linguistic comorbidities. Epilepsia 49, 1838–1846.

Carvalho, K., Faivre, E., Pietrowski, M.J., Marques, X., Gomez-Murcia, V., Deleau, A., Huin, V., Hansen, J.N., Kozlov, S., Danis, C., Temido-Ferreira, M., Coelho, J.E., Mériaux, C., Eddarkaoui, S., Gras, S.L., Dumoulin, M., Cellai, L., Landrieu, I., Chern, Y., Hamdane, M., Buée, L., Boutillier, A.L., Levi, S., Halle, A., Lopes, L.V., Blum, D., Bank, N.B., 2019. Exacerbation of C1q dysregulation, synaptic loss and memory deficits in tau pathology linked to neuronal adenosine A2A receptor. Brain 142, 3636–3654.

Casalia, M.L., Howard, M.A., Baraban, S.C., 2017. Persistent seizure control in epileptic mice transplanted with gamma-aminobutyric acid progenitors. Ann. Neurol. 82, 530–542.

Cavazos, J.E., Cross, D.J., 2006. The role of synaptic reorganization in mesial temporal lobe epilepsy. Epilepsy Behav. 8, 483–493.

Chen, Z.P., Zhao, X., Wang, S., Cai, R., Liu, Q., Ye, H., Wang, M.J., Peng, S.Y., Xue, W.X., Zhang, Y.X., Li, W., Tang, H., Huang, T., Zhang, Q., Li, L., Gao, L., Zhou, H., Hang, C., Zhu, J.N., Li, X., Liu, X., Cong, Q., Yan, C., 2025. GABA-dependent microglial elimination of inhibitory synapses underlies neuronal hyperexcitability in epilepsy. Nat. Neurosci.

Chu, Y., Jin, X., Parada, I., Pesic, A., Stevens, B., Barres, B., Prince, D.A., 2010. Enhanced synaptic connectivity and epilepsy in C1q knockout mice. Proc. Natl. Acad. Sci. 107, 7975–7980.

Clement, J.P., Ozkan, E.D., Aceti, M., Miller, C.A., Rumbaugh, G., 2013. SYNGAP1 links the maturation rate of excitatory synapses to the duration of critical-period synaptic plasticity. J. Neurosci. 33, 10447–10452.
Cobos, I., Calcagnotto, M.E., Vilaythong, A.J., Thwin, M.T., Noebels, J.L., Baraban, S.C., Rubenstein, J.L., 2005. Mice lacking Dlx1 show subtype-specific loss of interneurons, reduced inhibition and epilepsy. Nat. Neurosci. 8, 1059–1068.
Crunelli, V., Leresche, N., 2002. Childhood absence epilepsy: genes, channels, neurons and networks. Nat. Rev. Neurosci. 3, 371–382.
Cryan, J.F., Mombereau, C., Vassout, A., 2005. The tail suspension test as a model for assessing antidepressant activity: review of pharmacological and genetic studies in mice. Neurosci. Biobehav Rev. 29, 571–625.
Dejanovic, B., Wu, T., Tsai, M.C., Graykowski, D., Gandham, V.D., Rose, C.M., Bakalarski, C.E., Ngu, H., Wang, Y., Pandey, S., Rezzonico, M.G., Friedman, B.A., Edmonds, R., De Mazière, A., Rakosi-Schmidt, R., Singh, T., Klumperman, J., Foreman, O., Chang, M.C., Xie, L., Sheng, M., Hanson, J.E., 2022. Complement C1q-dependent excitatory and inhibitory synapse elimination by astrocytes and microglia in Alzheimer's disease mouse models. Nat. Aging 2, 837–850.
Dinocourt, C., Petanjek, Z., Freund, T.F., Ben-Ari, Y., Esclapez, M., 2003. Loss of interneurons innervating pyramidal cell dendrites and axon initial segments in the CA1 region of the hippocampus following pilocarpine-induced seizures. J. Comp. Neurol. 459, 407–425.
Fan, J., Dong, X., Tang, Y., Wang, X., Lin, D., Gong, L., Chen, C., Jiang, J., Shen, W., Xu, A., Zhang, X., Xie, Y., Huang, X., Zeng, L., 2023. Preferential pruning of inhibitory synapses by microglia contributes to alteration of the balance between excitatory and inhibitory synapses in the hippocampus in temporal lobe epilepsy. CNS Neurosci. Ther. 29, 2884–2900.
Glauser, T.A., Cnaan, A., Shinnar, S., Hirtz, D.G., Dlugos, D., Masur, D., Clark, P.O., Adamson, P.C., Team, C.A.E.S., 2013. Ethosuximide, valproic acid, and lamotrigine in childhood absence epilepsy: initial monotherapy outcomes at 12 months. Epilepsia 54, 141–155.
Gomez-Arboledas, A., Acharya, M.M., Tenner, A.J., 2021. The role of complement in synaptic pruning and neurodegeneration. Immunotargets Ther. 10, 373–386.
Hayashi, Y., Alamir, N., Sun, G., Tamagnini, F., Williams, C., Zheng, Y., 2024. An effective textured Novel Object Recognition Test (tNORT) for repeated measure of whisker sensitivity of rodents. Behav. Brain Res. 472, 115153.
Hensch, T.K., 2004. Critical period regulation. Annu Rev. Neurosci. 27, 549–579.
Holden, S.S., Grandi, F.C., Aboubakr, O., Higashikubo, B., Cho, F.S., Chang, A.H., Forero, A.O., Morningstar, A.R., Mathur, V., Kuhn, L.J., Suri, P., Sankaranarayanan, S., Andrews-Zwilling, Y., Tenner, A.J., Luthi, A., Aronica, E., Corces, M.R., Yednock, T., Paz, J.T., 2021. Complement factor C1q mediates sleep spindle loss and epileptic spikes after mild brain injury. Science 373, eabj2685.
Hong, S., Beja-Glasser, V.F., Nfonoyim, B.M., Frouin, A., Li, S., Ramakrishnan, S., Merry, K.M., Shi, Q., Rosenthal, A., Barres, B.A., Lemere, C.A., Selkoe, D.J., Stevens, B., 2016. Complement and microglia mediate early synapse loss in Alzheimer mouse models. Science 352, 712–716.
Howard, M.A., Baraban, S.C., 2016. Synaptic integration of transplanted interneuron progenitor cells into native cortical networks. J. Neurophysiol. 116, 472–478.
Hsieh, J.Y., Baraban, S.C., 2017. Medial ganglionic eminence progenitors transplanted into hippocampus integrate in a functional and subtype-appropriate manner. eNeuro 4.
Hunt, R.F., Baraban, S.C., 2015. Interneuron transplantation as a treatment for epilepsy. Cold Spring Harb. Perspect. Med. 5.
Hunt, R.F., Girskis, K.M., Rubenstein, J.L., Alvarez-Buylla, A., Baraban, S.C., 2013. GABA progenitors grafted into the adult epileptic brain control seizures and abnormal behavior. Nat. Neurosci. 16, 692–697.
Huusko, N., Römer, C., Ndode-Ekane, X.E., Lukasiuk, K., Pitkänen, A., 2015. Loss of hippocampal interneurons and epileptogenesis: a comparison of two animal models of acquired epilepsy. Brain Struct. Funct. 220, 153–191.
Jabarin, R., Netser, S., Wagner, S., 2022. Beyond the three-chamber test: toward a multimodal and objective assessment of social behavior in rodents. Mol. Autism 13, 41.
Jeong, Y., Lim, H.K., Kim, H., Lee, J., Lee, S., Suh, M., 2025. C1q neutralization during epileptogenesis attenuates complement-mediated synaptic elimination and epileptiform activity. Epilepsia.
Jiang, G.T., Shao, L., Kong, S., Zeng, M.L., Cheng, J.J., Chen, T.X., Han, S., Yin, J., Liu, W. H., He, X.H., Liu, Y.M., Gongga, L., Peng, B.W., 2021. Complement C3 Aggravates Post-epileptic Neuronal Injury Via Activation of TRPV1. Neurosci. Bull. 37, 1427–1440.
Kobayashi, M., Buckmaster, P.S., 2003. Reduced inhibition of dentate granule cells in a model of temporal lobe epilepsy. J. Neurosci. 23, 2440–2452.
Kraeuter, A.K., Guest, P.C., Sarnyai, Z., 2019. The open field test for measuring locomotor activity and anxiety-like behavior. Methods Mol. Biol. 1916, 99–103.
Kwon, C.S., Rafati, A., Ottman, R., Christensen, J., Kanner, A.M., Jetté, N., Newton, C.R., 2025. Psychiatric comorbidities in persons with epilepsy compared with persons without epilepsy: a systematic review and meta-analysis. JAMA Neurol. 82, 72–84.
Le Roux, M., Benallegue, N., Gueden, S., Rupin-Mas, M., Van Bogaert, P., 2024. Care of pharmaco-resistant absence seizures in childhood. Rev. Neurol. (Paris) 180, 251–255.
Lindquist, B.E., Timbie, C., Voskobiynyk, Y., Paz, J.T., 2023. Thalamocortical circuits in generalized epilepsy: pathophysiologic mechanisms and therapeutic targets. Neurobiol. Dis. 181, 106094.
Lui, H., Zhang, J., Makinson, S.R., Cahill, M.K., Kelley, K.W., Huang, H.Y., Shang, Y., Oldham, M.C., Martens, L.H., Gao, F., Coppola, G., Sloan, S.A., Hsieh, C.L., Kim, C.C., Bigio, E.H., Weintraub, S., Mesulam, M.M., Rademakers, R., Mackenzie, I.R., Seeley, W.W., Karydas, A., Miller, B.L., Borroni, B., Ghidoni, R., Farese, R.V., Paz, J. T., Barres, B.A., Huang, E.J., 2016. Progranulin deficiency promotes circuit-specific synaptic pruning by microglia via complement activation. Cell 165, 921–935.
Ma, Y., Ramachandran, A., Ford, N., Parada, I., Prince, D.A., 2013. Remodeling of dendrites and spines in the C1q knockout model of genetic epilepsy. Epilepsia 54, 1232–1239.
Madeshiya, A.K., Whitehead, C., Tripathi, A., Pillai, A., 2022. C1q deletion exacerbates stress-induced learned helplessness behavior and induces neuroinflammation in mice. Transl. Psychiatry 12, 50.
Nandi, A., Virmani, G., Barve, A., Marathe, S., 2021. DBscorer: an open-source software for automated accurate analysis of rodent behavior in forced swim test and tail suspension test. eNeuro 8.
Park, Y.G., Sohn, C.H., Chen, R., McCue, M., Yun, D.H., Drummond, G.T., Ku, T., Evans, N.B., Oak, H.C., Trieu, W., Choi, H., Jin, X., Lilascharoen, V., Wang, J., Truttmann, M.C., Qi, H.W., Ploegh, H.L., Golub, T.R., Chen, S.C., Frosch, M.P., Kulik, H.J., Lim, B.K., Chung, K., 2018. Protection of tissue physicochemical properties using polyfunctional crosslinkers. Nat. Biotechnol.
Paterno, R., Vu, T., Hsieh, C., Baraban, S.C., 2024. Host brain environmental influences on transplanted medial ganglionic eminence progenitors. Sci. Rep. 14, 3610.
Patrikelis, P., Angelakis, E., Gatzonis, S., 2009. Neurocognitive and behavioral functioning in frontal lobe epilepsy: a review. Epilepsy Behav. 14, 19–26.
Presumey, J., Bialas, A.R., Carroll, M.C., 2017. Complement system in neural synapse elimination in development and disease. Adv. Immunol. 135, 53–79.
Ramaswamy, S., Colangelo, C., Muller, E.B., 2017. Distinct activity profiles of somatostatin-expressing interneurons in the neocortex. Front Cell Neurosci. 11, 273.
Righes Marafiga, J., Vendramin Pasquetti, M., Calcagnotto, M.E., 2021. GABAergic interneurons in epilepsy: more than a simple change in inhibition. Epilepsy Behav. 121, 106935.
Rossignol, E., Kruglikov, I., van den Maagdenberg, A.M., Rudy, B., Fishell, G., 2013. CaV 2.1 ablation in cortical interneurons selectively impairs fast-spiking basket cells and causes generalized seizures. Ann. Neurol. 74, 209–222.
Samalens, L., Beets, C., Courivaud, C., Kahane, P., Depaulis, A., 2025. Comorbidities in the mouse model of temporal lobe epilepsy induced by intrahippocampal kainate. Epilepsia.
van Schaarenburg, R.A., Magro-Checa, C., Bakker, J.A., Teng, Y.K., Bajema, I.M., Huizinga, T.W., Steup-Beekman, G.M., Trouw, L.A., 2016. C1q deficiency and neuropsychiatric systemic lupus erythematosus. Front Immunol. 7, 647.
Schartz, N.D., Tenner, A.J., 2020. The good, the bad, and the opportunities of the complement system in neurodegenerative disease. J. Neuroinflamm. 17, 354.
Schartz, N.D., Wyatt-Johnson, S.K., Price, L.R., Colin, S.A., Brewster, A.L., 2018. Status epilepticus triggers long-lasting activation of complement C1q-C3 signaling in the hippocampus that correlates with seizure frequency in experimental epilepsy. Neurobiol. Dis. 109, 163–173.
Schulz, K., Trendelenburg, M., 2022. C1q as a target molecule to treat human disease: What do mouse studies teach us? Front Immunol. 13, 958273.
Sierra, D.P., Tripathi, A., Pillai, A., 2022. Dysregulation of complement system in neuropsychiatric disorders: a mini review. Biomark. Neuropsychiatry 7.
Silberberg, G., Markram, H., 2007. Disynaptic inhibition between neocortical pyramidal cells mediated by Martinotti cells. Neuron 53, 735–746.
Stephan, A.H., Madison, D.V., Mateos, J.M., Fraser, D.A., Lovelett, E.A., Coutellier, L., Kim, L., Tsai, H.H., Huang, E.J., Rowitch, D.H., Berns, D.S., Tenner, A.J., Shamloo, M., Barres, B.A., 2013. A dramatic increase of C1q protein in the CNS during normal aging. J. Neurosci. 33, 13460–13474.
Stevens, B., Allen, N.J., Vazquez, L.E., Howell, G.R., Christopherson, K.S., Nouri, N., Micheva, K.D., Mehalow, A.K., Huberman, A.D., Stafford, B., Sher, A., Litke, A.M., Lambris, J.D., Smith, S.J., John, S.W., Barres, B.A., 2007. The classical complement cascade mediates CNS synapse elimination. Cell 131, 1164–1178.
Tau, G.Z., Peterson, B.S., 2010. Normal development of brain circuits. Neuropsychopharmacology 35, 147–168.
Tenner, A.J., 2020. Complement-mediated events in Alzheimer's disease: mechanisms and potential therapeutic targets. J. Immunol. 204, 306–315.
Tenner, A.J., Stevens, B., Woodruff, T.M., 2018. New tricks for an ancient system: physiological and pathological roles of complement in the CNS. Mol. Immunol. 102, 3–13.
Thomas, A., Burant, A., Bui, N., Graham, D., Yuva-Paylor, L.A., Paylor, R., 2009. Marble burying reflects a repetitive and perseverative behavior more than novelty-induced anxiety. Psychopharmacol. (Berl.) 204, 361–373.
Vinti, V., Dell'Isola, G.B., Tascini, G., Mencaroni, E., Cara, G.D., Striano, P., Verrotti, A., 2021. Temporal lobe epilepsy and psychiatric comorbidity. Front Neurol. 12, 775781.
Wang, C., Liu, J.Y., Su, L.D., Wang, X.T., Bian, Y.P., Wang, Z.X., Ye, L.Y., Lu, X.J., Zhou, L., Chen, W., Yang, W., Liu, J., Wang, L., Shen, Y., 2025. GABAergic progenitor cell graft rescues cognitive deficits in fragile x syndrome mice. Adv. Sci. 12, e2411972.
Wei, Y., Chen, T., Bosco, D.B., Xie, M., Zheng, J., Dheer, A., Ying, Y., Wu, Q., Lennon, V. A., Wu, L.J., 2021. The complement C3-C3aR pathway mediates microglia-astrocyte interaction following status epilepticus. Glia 69, 1155–1169.
Whitelaw, B.S., 2018. Microglia-mediated synaptic elimination in neuronal development and disease. J. Neurophysiol. 119, 1–4.
Wilton, D.K., Mastro, K., Heller, M.D., Gergits, F.W., Willing, C.R., Fahey, J.B., Frouin, A., Daggett, A., Gu, X., Kim, Y.A., Faull, R.L.M., Jayadev, S., Yednock, T., Yang, X.W., Stevens, B., 2023. Microglia and complement mediate early corticostriatal synapse loss and cognitive dysfunction in Huntington's disease. Nat. Med. 29, 2866–2884.
Wu, X., Gao, Y., Shi, C., Tong, J., Ma, D., Shen, J., Yang, J., Ji, M., 2023. Complement C1q drives microglia-dependent synaptic loss and cognitive impairments in a mouse model of lipopolysaccharide-induced neuroinflammation. Neuropharmacology 237, 109646.

Wyatt, S.K., Witt, T., Barbaro, N.M., Cohen-Gadol, A.A., Brewster, A.L., 2017. Enhanced classical complement pathway activation and altered phagocytosis signaling molecules in human epilepsy. Exp. Neurol. 295, 184–193.
Yilmaz, M., Yalcin, E., Presumey, J., Aw, E., Ma, M., Whelan, C.W., Stevens, B., McCarroll, S.A., Carroll, M.C., 2021. Overexpression of schizophrenia susceptibility factor human complement C4A promotes excessive synaptic loss and behavioral changes in mice. Nat. Neurosci. 24, 214–224.
Yuzaki, M., 2017. The C1q complement family of synaptic organizers: not just complementary. Curr. Opin. Neurobiol. 45, 9–15.
Zhang, W., Chen, Y., Pei, H., 2023. C1q and central nervous system disorders. Front Immunol. 14, 1145649.
Zipancic, I., Calcagnotto, M.E., Piquer-Gil, M., Mello, L.E., Alvarez-Dolado, M., 2010. Transplant of GABAergic precursors restores hippocampal inhibitory function in a mouse model of seizure susceptibility. Cell Transpl. 19, 549–564.